The Li isotope composition of marine biogenic carbonates: Patterns and Mechanisms

Mathieu Dellinger, A. Joshua West, Guillaume Paris, Jess F Adkins, Philip Pogge von Strandmann, Clemens V Ullmann, Robert A. Eagle, Pedro Freitas, Marie-Laure Bagard, Justin B Ries, et al.

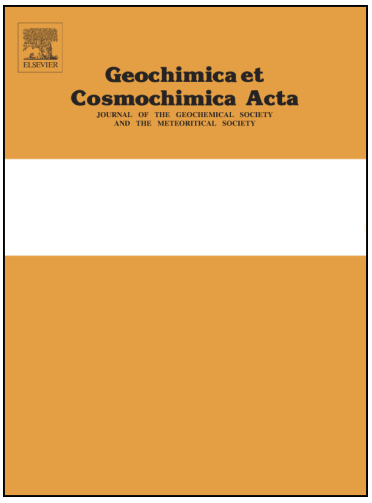

The Li isotope composition of marine biogenic carbonates: Patterns and Mechanisms

Mathieu Dellinger, A. Joshua West, Guillaume Paris, Jess F. Adkins, Philip Pogge von Strandmann, Clemens V. Ullmann, Robert A. Eagle, Pedro Freitas, Marie-Laure Bagard, Justin B. Ries, Frank A. Corsetti, Alberto Perez-Huerta, Anthony R. Kampf

PII: S0016-7037(18)30165-0
DOI: https://doi.org/10.1016/j.gca.2018.03.014
Reference: GCA 10708

To appear in: *Geochimica et Cosmochimica Acta*

Received Date: 30 August 2017
Accepted Date: 10 March 2018

Please cite this article as: Dellinger, M., Joshua West, A., Paris, G., Adkins, J.F., Pogge von Strandmann, P., Ullmann, C.V., Eagle, R.A., Freitas, P., Bagard, M-L., Ries, J.B., Corsetti, F.A., Perez-Huerta, A., Kampf, A.R., The Li isotope composition of marine biogenic carbonates: Patterns and Mechanisms, *Geochimica et Cosmochimica Acta* (2018), doi: https://doi.org/10.1016/j.gca.2018.03.014

The Li isotope composition of marine biogenic carbonates: Patterns and Mechanisms

Authors:

Mathieu Dellinger[1]*, A. Joshua West[1], Guillaume Paris[2,3], Jess F. Adkins[2], Philip Pogge von Strandmann[4], Clemens V. Ullmann[5], Robert A. Eagle[6,7,8], Pedro Freitas[9], Marie-Laure Bagard[10], Justin B. Ries[11], Frank A. Corsetti[1], Alberto Perez-Huerta[12], Anthony R. Kampf[13]

1. Department of Earth Sciences, University of Southern California, Los Angeles, USA
2. Division of Geological and Planetary Sciences, California Institute of Technology, Pasadena, CA, USA
3. Centre de Recherches Pétrographiques et Géochimiques (CRPG), UMR 7358, CNRS-Université de Lorraine
4. London Geochemistry and Isotope Centre, Institute of Earth and Planetary Sciences, University College London and Birkbeck, University of London, Gower Street, London, WC1E 6BT, UK
5. University of Exeter, Camborne School of Mines & Environment and Sustainability, Institute, Penryn Campus, Penryn, TR10 9FE, UK.
6. Institute of the Environment and Sustainability, University of California, Los Angeles, LaKretz Hall, 619 Charles E Young Dr E #300, Los Angeles, CA 90024, USA
7. Atmospheric and Oceanic Sciences Department, University of California – Los Angeles, Maths Science Building, 520 Portola Plaza, Los Angeles, CA 90095, USA
8. Université de Brest, UBO, CNRS, IRD, Ifremer, Institut Universitaire Européen de la Mer, LEMAR, Rue Dumont d'Urville, 29280, Plouzané, France
9. Divisao de Geologia e Georecursos Marinhos, Instituto Portugues do Mar e da Atmosfera (IPMA), Av. de Brasilia s/n, 1449-006 Lisbon, Portugal
10. Institut des Sciences de la Terre d'Orléans (ISTO), UMR 7327, CNRS, Université d'Orléans, BRGM, 1A, rue de la Férollerie, 45071 Orléans Cedex 2, France
11. Department of Marine and Environmental Sciences, Marine Science Center, Northeastern University, Nahant, MA 01908, United States
12. Department of Geological Sciences, The University of Alabama, Tuscaloosa, AL 35487, USA
13. Mineral Sciences Department, Natural History Muséum of Los Angeles County, 900 Exposition Boulevard, Los Angeles, CA 90007, USA

* Corresponding author: now at Durham University, Geography Department, South Road, Durham, UK

ABSTRACT

Little is known about the fractionation of Li isotopes during formation of biogenic carbonates, which form the most promising geological archives of past seawater composition. Here we investigated the Li isotope composition (δ^7Li) and Li/Ca ratios of organisms that are abundant in the Phanerozoic record, mollusks (mostly bivalves), echinoderms, and brachiopods. The measured samples include (i) modern calcite and aragonite shells from variable species and natural environments (13 mollusk samples, 5 brachiopods and 3 echinoderms), and (ii) shells from organisms grown under controlled conditions at various temperatures. When possible, the mollusk shell ultrastructure was micro-sampled in order to assess intra-shell heterogeneity. In this paper, we systematically characterize the respective influence of mineralogy, temperature, and biological processes on the δ^7Li and Li/Ca of these shells and compare with published data for other taxa (foraminifera and corals).

Aragonitic mollusks have the lowest δ^7Li, ranging from +16 to +22‰, echinoderms have constant δ^7Li of about +24‰, brachiopods have δ^7Li of +25 to +28‰, and finally calcitic mollusks have the largest range and highest δ^7Li values, ranging from +25‰ to +40‰. Measured brachiopods have similar δ^7Li compared to inorganic calcite precipitated from seawater (δ^7Li of +27 to +29‰), indicating minimum influence of vital effects, as also observed for other isotope systems and making them a potentially viable proxy of past seawater composition. Calcitic mollusks, on the contrary, are not a good archive for seawater paleo–δ^7Li because many samples have significantly higher δ^7Li values than inorganic calcite and display large inter-species variability, which suggest large vital effects. In addition, we observe very large intra-shell variability, in particular for mixed calcite-aragonite shells (over 20‰ variability), but also in mono-mineralic shells (up to 12‰ variability). Aragonitic bivalves have less variable δ^7Li (7‰ variability) compared to calcitic mollusks, but with significantly lower δ^7Li compared to inorganic aragonite, indicating the existence of vital effects. Bivalves grown at various temperatures show that temperature has only a minor influence on fractionation of Li isotopes during shell precipitation. Interestingly, we observe a strong correlation (R^2=0.83) between the Li/Mg ratio in bivalve *Mytilus edulis* and temperature with potential implications for paleo-temperature reconstructions.

Finally, we observe a negative correlation between the δ^7Li and both the Li/Ca and Mg/Ca ratio of calcite mollusks, which we relate to biomineralization processes. To explain this correlation, we propose preferential removal of ^{6}Li from the calcification site of calcite

mollusks by physiological processes corresponding to the regulation of the amount of Mg in the calcifying medium. We calculate that up to 80% of the initial Li within the calcification site is removed by this process, leading to high δ^7Li and low Li/Ca in some calcite mollusks specimens. Collectively, these results suggest that Mg (and thus [Li]) are strongly biologically controlled within the calcifying medium of calcite mollusks. More generally, the results of this study show that brachiopods are suitable targets for future work on the determination of paleo-seawater Li isotope composition—an emerging proxy for past weathering and hydrothermal processes.

1. INTRODUCTION

A growing body of evidence suggests that the Li isotope composition of seawater may be a promising proxy for tracing past weathering and hydrothermal conditions at the Earth's surface, because the primary inputs of Li to the oceans are from rivers and the high-temperature hydrothermal flux from ocean ridges (Chan et al., 1992; Hathorne and James, 2006; Huh et al., 1998; Misra and Froelich, 2012). Furthermore, the residence time of Li in the ocean is about 1–3 Ma, and the marine Li isotopic composition ($\delta^7\text{Li} = [(^7\text{Li}/^6\text{Li})/(^7\text{Li}/^6\text{Li})_{\text{L-SVEC}} - 1] \times 1000$; expressed in ‰) and concentration are spatially uniform (Angino and Billings 1966). Published Li isotope records in foraminifera (Hathorne and James, 2006; Misra and Froelich, 2012) and bulk carbonates (Lechler et al., 2015; Pogge von Strandmann et al., 2013; Pogge von Strandmann et al., 2017) are characterized by large (several per mil) δ^7Li variations. These changes have been attributed to past changes in weathering congruency, intensity, or rates (Bouchez et al., 2013; Froelich and Misra, 2014; Li and West, 2014; Wanner et al., 2014).

The relationship between Li isotope fractionation and chemical weathering on continents has been well-studied, and although details are still debated, general trends are understood (Bagard et al., 2015; Dellinger et al., 2015; Dellinger et al., 2017; Huh et al., 2001; Pogge von Strandmann and Henderson, 2015; Wanner et al., 2014). Dissolved Li transported to the oceans is primarily derived from the weathering of silicate rocks (Huh et al., 2001; Kısakűrek et al., 2005), which generates alkalinity and, unlike carbonate weathering, sequesters CO_2 in carbonate rocks over geologic timescales (>10-100 kyrs). Li isotopes are strongly fractionated during water-rock interaction, with ^{6}Li being preferentially

incorporated into clay minerals while ^{7}Li is concentrated in the dissolved phase (Huh et al., 1998; Pistiner and Henderson, 2003; Chan et al., 1992). As a result, dissolved riverine $\delta^{7}Li$ varies as a function of the ratio of primary mineral dissolution to secondary mineral formation (e.g. Pogge von Strandmann and Henderson, 2015), and the evolution of $\delta^{7}Li$ and Li/Ca ratios of the ocean may provide information about paleo-weathering regimes.

Reconstructing Li isotopic composition of seawater requires a sedimentary archive and carbonates have been a preferred target so far (e.g. Misra and Froelich, 2012; Pogge von Strandmann et al., 2013; Vigier et al., 2007). However, the fractionation of Li isotopes during biogenic carbonate precipitation has been explored mainly in foraminifera and corals but is less understood in other organisms. Laboratory experiments inform general understanding of Li incorporation into inorganic carbonates. In aragonite, Li^{+} is thought to substitute for Ca^{2+} in the mineral lattice, whereas in calcite, Li^{+} occupies an interstitial location (Okumura and Kitano, 1986). The Li/Ca ratio of inorganic carbonates is influenced by the Li/Ca ratio and/or the Li concentration of the fluid from which it precipitates (Gabitov et al., 2011; Marriott et al., 2004b, 2004a). The Li/Ca ratio of inorganic calcite decreases with increasing temperature (Marriott et al., 2004a,b). An increase in Li/Ca with salinity was also observed for calcite but not for aragonite (Marriott et al., 2004b) but the Li/Ca ratio of inorganic aragonite increases with precipitation rate (Gabitov et al., 2011). In addition, the isotopic fractionation factor between inorganic calcium carbonate and solution is strongly dependent upon the carbonate mineralogy, with the fractionation factor between inorganic aragonite and seawater, $\alpha_{aragonite\text{-}seawater}$ = 0.988 to 0.993 (corresponding to a $\Delta_{aragonite\text{-}seawater}$ of –7 to –12‰) and the fractionation factor between inorganic calcite and seawater $\alpha_{calcite\text{-}seawater}$ = 0.998 to 0.995 ($\Delta_{calcite\text{-}seawater}$ of –2 to –5‰; Marriott et al., 2004a,b; Gabitov et al., 2011).

A number of studies have investigated the Li/Ca ratio of biogenic carbonates, showing that the incorporation of lithium depends upon various parameters that include temperature, salinity, growth rate, carbonate ion concentration, dissolved Li concentration, and biology (also called “vital effects”). Temperature appears to be a major control on the Li/Ca ratio of brachiopods, which show increasing Li/Ca with decreasing temperature (Delaney et al., 1989), similar to that observed for inorganic calcite. However, no systematic trend between Li/Ca and temperature has been observed for other biogenic carbonates. Instead, culture experiments and core top studies have shown that the Li/Ca ratio of foraminifera is influenced by the solution Li/Ca ratio, DIC concentration, and possibly the growth rate (Delaney et al., 1985; Hall and Chan, 2004; Hathorne and James, 2006; Lear and Rosenthal,

2006; Vigier et al., 2015). In contrast, the Li/Mg ratio of corals and foraminifera is more strongly related to temperature than Li/Ca and has been recently proposed as being a reliable proxy for ocean temperature (Bryan and Marchitto, 2008; Case et al., 2010; Montagna et al., 2014; Rollion-Bard and Blamart, 2015; Fowell et al., 2016). The Li/Ca ratio of mollusks might be controlled by a combination of vital effects, growth rate, changes in ocean productivity, and/or dissolution of riverine fine sediments within the ocean (Füllenbach et al., 2015; Thébault et al., 2009; Thébault and Chauvaud, 2013).

In contrast to Li elemental ratios, Li isotope ratios have been investigated only in modern foraminifera and corals. Modern corals have Li isotopic composition ranging from +17 to +25‰ (Marriott et al., 2004a,b; Rollion-Bard et al., 2009), significantly fractionated relative to seawater but with an average δ^7Li similar to inorganic aragonite (around +19‰). The intra-specimen variability for corals is relatively low, less than ±2‰, but small systematic differences exists between species (Rollion-Bard et al., 2009). Present-day planktic foraminifera δ^7Li range between +27 and +31‰ (Hall et al., 2005; Hathorne and James, 2006; Misra and Froelich, 2012) with a median value of 30‰, very close to modern seawater (31‰), making them targets for past work reconstructing the Li isotope composition of the Cenozoic ocean (Hathorne and James, 2006; Misra and Froelich, 2012). However, Li isotopic fractionation in foraminifera may depend upon seawater dissolved inorganic carbon (DIC) concentration of seawater (Vigier et al., 2015). In addition, well-preserved planktic foraminifera are not very abundant in the geological record prior to the Cenozoic (Wilkinson, 1979). Finally, Ullmann et al. (2013b) for belemnite and Pogge von Strandmann et al., (2017) for brachiopods have shown that the shell of these organisms may preserve Li isotope composition of the ocean over geological timescales.

In this study, we focus mainly on characterizing the δ^7Li and Li/Ca of these organisms (particularly bivalves and brachiopods), since these may be some of the most important Phanerozoic paleoenvironmental bioarchives, and, also present a few measurements of echinoderm. Bivalves, brachiopods, and echinoderms are present in widely distributed habitats in the modern-day ocean, are often well-preserved during diagenesis, and are abundant in the Phanerozoic record (Immenhauser et al., 2016; Veizer et al., 1999; Wilkinson, 1979). Prior studies have reported Li isotope data on Ordovician brachiopods (Pogge von Strandmann et al., 2017), Li/Ca values of modern bivalves and brachiopods (Delaney et al., 1989; Füllenbach et al., 2015; Thébault et al., 2009; Thébault and Chauvaud, 2013), but no Li isotope data on modern bivalves and brachiopods. Here we test the influence of temperature,

mineralogy and biology on Li isotopic composition and Li/Ca ratio on a set of mollusk, brachiopod and echinoderm samples from various environments, in order to evaluate the suitability of these taxa to reconstructing past $\delta^7Li_{seawater}$.

2. ORIGIN OF THE SAMPLES AND SAMPLING STRATEGY

Two types of samples have been investigated: (i) shells from modern marine organisms corresponding to a wide range of mineralogy, species, and locations; and (ii) shells grown from controlled culture experiments at various temperatures.

2.1. Field-collected modern shells

Modern shell samples were retrieved from the LA County Natural History Museum collections, supplemented with miscellaneous other specimens. All mollusk samples from this study, except the gastropod *Turritella*, are bivalves (n=17 specimens). They come from 13 species comprising oysters, clams, mussels, and scallops. We also analyzed 5 brachiopod and 3 echinoderm specimens, each from different species. These shells come from a wide range of marine environments from cold to warm sea surface temperature (–1 to 30°C). The location and characteristics of the specimens are summarized in Table (1) and Fig (1). We extracted the main seawater parameters (sea surface temperature – SST, salinity, alkalinity), including both annual averages and, when possible, specifically for the growth interval of the shells (average of the 3 months having the highest SST). We used the World Ocean Atlas 2013 for SST and salinity (Locarnini et al., 2013) and GLODAPv2 database for the alkalinity (Olsen et al., 2016), or specified references when more accurate data were available. Because of uncertainty regarding the sampling location, we attribute a relatively large uncertainty to these ocean parameters.

Field-collected shells were cleaned in an ultrasonic bath with distilled water, cut, and drilled. The sampling strategy was intended to simultaneously sample a large (20-30 mg), representative “bulk” sample in the middle of the shell while also targeting some micro-scale samples, using a micro-mill, in order to investigate possible intra-shell variability (Fig. 2).

We studied four different specimens of oysters (*Crassostrea gigas)* from four different localities spanning a wide range of ocean temperature (12 to 27°C). The shell of *Crassostrea gigas* is predominantly composed of calcite with two types of mineralogical structure, the "chalky structure" and "foliate layers" (Carriker et al., 1980; Carriker and Palmer, 1979;

Ullmann et al., 2010, 2013a). The chalky structure is composed of a 3D network while foliate layers are elongated calcite crystals. "Bulk" samples of about 20 mg of mixed calcite were sampled in the middle and outer layer of specimens collected in Washington and California (USA) and Ecuador. The fourth specimen was collected in the North Sea in the List basin and has been previously investigated at small scale for other chemical proxies (Ullmann et al., 2013a, 2010). Specific foliate layers and chalky structure were micro-sampled (see Ullmann et al., 2010 for details about the sampling protocol). We also determined the growth temperature for the North Sea oyster sample using calcite $\delta^{18}O$, following Ullmann et al. (2010; 2013a) using an average $\delta^{18}O$ value for the List basin seawater of –1.3‰ (V-SMOW).

Scallop samples are from two distinct genera (*Chlamys* and *Adamussium*). Three different *Chlamys* species were investigated: *Chlamys cheritata* (Alaska), *Chlamys hastata* (California), and *Laevichlamys squamosa* (Philippines). For *Adamussium*, we studied one specimen of *Adamussium colbecki* from Antarctica (partly described in Eagle et al., (2013). One sample of 20 mg for each of these species was collected by milling the middle of the shell, and these samples thus correspond to a mix of the prismatic and nacreous layers.

Two *Mytilus californianus* mussel specimens but from different locations, the USA (Washington State) and Mexico, were also studied. The shell of *Mytilus californianus* is composed of a calcite prismatic outer layer and an aragonite nacreous inner layer. Because of this mineralogical heterogeneity, both specimens were micro-drilled at various locations of the shell in order to sample the inner or outer layer separately.

Clam specimens studied here comprise three genera (*Chione, Tridacna* and *Laternula*). *Chione* specimens (mostly composed of aragonite) are from three different species: *Chione californiensis* (California), *Chione subimbricata* (Costa Rica), and *Chione subrugosa* (Peru). The two *Tridacna* species studied were *Tridacna gigas* (Costa Rica) and *Tridacna maxima* (Mariana island), both with a shell of pure aragonite. One shell sample of 20 mg for each of these species was collected by milling the middle of the shell, and specific inner and outer layers were also sampled to test for intra-shell variability.

Five specimens each from different species of calcitic brachiopods were investigated in this study. These samples include the species *Campages mariae* (Aliguay Island, Philippines), *Laqueus rubellus* (Sagami Bay, Japan), *Terebratalia transversa* (Friday Harbor, Washington State, USA), *Notosaria nigricans* (South Island, New Zealand), and *Frenulina sanguinolenta* (Mactan Island, Philippines). These Brachiopods have primary and secondary shell layers (both calcite, with different ultrastructure). Unlike the primary layer and the outer part of the secondary layer, the innermost part of the secondary layer is characterized by negligible vital

effects for C and O isotopes (Cusack et al., 2012; Penman et al., 2013; Ullmann et al., 2017; Auclair et al., 2003; Parkinson et al., 2005). We primarily sampled bulk mixed layer samples (corresponding mostly to the secondary layer) in this study. Approximately 20 mg of bulk powder was collected from each species except for *Terebratulina retusa*, which was sampled from various portions of the shell to test for intra-shell variability of Li isotope composition.

Three species of sea urchins (High-Mg calcite) were collected from California waters, *Strongylocentrotus fransiscanus*, *Strongylocentrotus purpuratus* and *Dendraster* sp. and a large 30 mg bulk powder was collected for each of the samples.

2.2. Cultured shells

Two calcite bivalve species, *Mytilus edulis* and *Pecten maximus* (Freitas et al., 2008) and one aragonite bivalve (*Mercenaria mercenaria*) were experimentally grown at various temperatures. Details about the culture experiments for *Mytilus edulis* and *Pecten maximus* are available in (Freitas et al., 2012, 2008, 2006). *Mercenaria mercenaria* was grown at temperature between 15 and 30°C, *Mytilus edulis* between 10.7 and 20.2°C and *Pecten maximus* between 10.8 and 20.2°C. Only the outer layer of the shells was sampled. The thin inner layer of *Mytilus edulis* was milled out when present (from the pallial line towards the umbo) before sampling from the outer surface. For *Pecten maximus*, the shell was sampled from the outer cross-lamellar layer, close to the margin and away from the inner layer and myostracum. Surface features like growth disturbances and the striae that tend to show a disturbed arrangement of crystals and high Mg/Ca, Sr/Ca and Mn/Ca ratios (Freitas et al., 2006) were included in the sampling.

3. ANALYTICAL METHODS

3.1. Mineralogy

The proportion of aragonite versus calcite for the vast majority of the powdered samples was measured at the Natural History Museum of Los Angeles County with a R-AXIS RAPID II X-ray diffraction system. Whole-pattern-fitting, implemented in JADE 2010 (Materials Data, Inc.), was used to analyze the X-ray powder diffraction patterns. The precision for this method is about ±5%.

3.2. Leaching and dissolution of the samples

Since lithium concentrations in carbonates are generally very low (lower than 1 ppm), carbonate samples are sensitive to contamination by other phases during dissolution, particularly silicate minerals (Vigier et al., 2007). All samples were therefore subjected to a pre-leach following a method modified from Saenger and Wang (2014), to remove exchangeable ions using 1N ammonium acetate followed by 3 rinses with milliQ (millipore) water. The samples were then digested in dilute hydrochloric acid (HCl 0.05N) for 1 hour. The volume of acid used for digestion was calculated to dissolve about 95% of the sample in order to minimize the leaching of non-carbonate phases. After 1 hour, the supernatant was collected while the sample residue was weighed in order to determine the yield of the digestion. For the great majority of samples, the yield for the digestion was between 90 and 100%. As discussed below, Al/Ca ratios were measured in order to confirm the absence of aluminosilicate-derived solutes in the leachate.

3.3. Trace element measurements

Ratios of trace elements Li, Mg, Sr, Al, Mn, Fe relative to Ca were measured using a Thermo Scientic Element 2 inductively coupled plasma mass spectrometer (ICP-MS) at the University of Southern California (USC) following a method adapted from Misra et al., (2014). All samples and standards were measured at a Ca concentration of 50 ppm. Li, Mg, Sr, Al concentrations were measured at low mass resolution whereas Fe and Mn were measured at medium mass resolution. The instrument was first conditioned for 1 hour with a solution of 50 ppm Ca. A set of 10 multi-elemental calibration standards was measured at the beginning of the run, and a bracketing standard solution was measured every 5 to 10 samples to correct for the drift of the signal. Accuracy and precision of analyses were checked using the aragonite reference material FEBS-1 (NRC) and in-house prepared standard solutions matching typical calcium carbonate chemical composition. Analytical precision was between 5 and 15%, depending on the element and the concentration (see details in supplementary materials).

3.4. Lithium isotopes

Lithium was separated from the matrix by ion-exchange chromatography using a method modified from James and Palmer, (2000). The dissolved calcium carbonate fraction was passed through a column containing 4mL of Biorad AG50W X-12 (200–400 mesh) resin. The Li fraction was eluted with 0.5N HCl (elution volume of about 13.5 mL) and evaporated to dryness at a temperature of 90-100°C. Purified samples were kept until measurement as

solid salts in Teflon beakers and subsequently dissolved in 5% HNO_3 for mass spectrometry analysis. Lithium isotope ratios were measured on a Thermo Neptune MC ICP-MS at Caltech, using a Cetac Aridus desolvator as an introduction system. Samples were measured following a standard-sample bracketing method with the commonly used L-SVEC standard (Flesch et al., 1973). The method comprised 50 cycles of 4 seconds for both standards and samples. Typical sensitivity was ~30 pA (about 3V) for 10 ng/g Li solution. Most of the samples were measured at concentrations ranging from 5 to 10 ng/g, the smallest samples measured at 1 or 2 ng/g. A clean acid measurement was measured before and after each sample and standard and subtracted to correct for the background contribution. Each sample was typically measured twice in a row. Accuracy and reproducibility of the isotopic measurements were checked through repeated analyses of seawater, with long-term average δ^7Li = +30.9 ± 0.8‰ (2s, n=63 separations and measurements) and L-SVEC solutions passed through columns giving δ^7Li = -0.1 ± 0.8‰ (2s, n=25 separations and measurements). We therefore consider that the external measurement precision is ±1‰. More informations about the analytical method are available in the supplementary materials.

The samples of the oyster *Crassostrea gigas* from the List Basin were purified using a similar technique (Pogge von Strandmann et al., 2013, Pogge von Strandmann and Henderson, 2015), where the dissolved calcium carbonate fraction was passed through a 2-stage cation exchange procedure with columns containing Biorad AG50W X-12 (200-400 mesh) resin. The first column contained 2.4ml resin, and the second column 0.5ml. In both cases the Li fraction was eluted using 0.2M HCl. Analyses were performed on a Nu Instruments HR MC-ICP-MS at Oxford, with a ^7Li sensitivity of ~18 pA for a 20 ng/ml solution at an uptake rate of 75 µl/min. Analyses consisted of three separate repeats of 10 ratios (10 s total integration time), for a total duration of 300 s/sample during each analytical session. Precision and accuracy were assessed by multiple analyses of N. Atlantic seawater, with a long-term value and reproducibility of +31.2 ± 0.6‰ (2 s.d. n=61). Other carbonate (JLs-1 and in-house marl standard) and rock (BCR-2 and SGR-1) standards are reported in Pogge von Strandmann et al. (2013, 2017). The total procedural blank for Li isotopes is effectively undetectable (<0.005 ng Li).

4. RESULTS

4.1. Sample mineralogy

The sample set from this study included shells composed of pure calcite, aragonite, high-Mg calcite and mixtures of these minerals. Mineralogy was measured when possible on the same powder used for Li isotope analysis (see table 1). Pure calcite specimens (over 95% calcite) included oysters (*C. gigas*), scallops (*P. maximus*, *C. cheritata* and *C. hastata*), and brachiopod samples. Pure aragonitic skeletal material from this study included clams (*T. gigas* and *T. maxima*) and gastropods (*Turritella*). All other measured specimens had a mixed mineralogy, and, for this reason, were micro-sampled at specific locations on the shells to obtain mineralogically pure phases. The drilled *C. squamosa* sample contained about 30% aragonite. *Chione* samples were primarly composed of aragonite, with a lesser proportion of calcite (1 to 46%). The mineralogy of *Mytilus californianus* shell samples ranged from pure calcite to pure aragonite. The mineralogy of experiment culture samples was not measured but inferred from previous studies (e.g., Ries, 2011; Freitas et al., 2006, 2008) to be either pure calcite (*Mytilus edulis, Pecten maximus*) or pure aragonite (*Mercenaria mercenaria*). The mineralogy for specific layers of the oyster sample was not measured either but is assumed to be pure calcite (Ullmann et al., 2010). In the following, we refer to “calcite” or “aragonite” for samples having more than 95% calcite and aragonite, respectively, with other samples being classified as "mixed".

4.2. Major and trace element ratios

We use minor and major element ratios, along with mineralogical data, to characterize the samples from this study. In general, aragonite has higher Sr and lower Mg concentrations than calcite (Dodd, 1967; Milliman et al., 1974). Our dataset is consistent with these observations. The Mg/Ca ratios of the current dataset span over two orders of magnitude, ranging from 0.3 to 109 mmol.mol^{-1} (Fig 3). Aragonite and mixed shell samples have lower Mg/Ca values (0.3 to 8.0 mmol.mol^{-1}) compared to low-magnesium calcite (LMC; with Mg/Ca of 1.0 to 20.0 mmol.mol^{-1}). The sea urchin samples (HMC) have the highest Mg/Ca ratios within this dataset, ranging from 80 to 109 mmol.mol^{-1}. The Mg/Ca values of the shells of *Pecten maximus* and *Mytilus edulis* agree well with previously published values from the literature (Freitas et al., 2009, 2008, 2006). The Sr/Ca values range from 0.5 to 2.5 mmol.mol^{-1}, with aragonite and high-magnesium calcite (HMC) samples from this study having higher Sr/Ca compared to LMC. The Mg/Ca and Sr/Ca values of our samples are in the range of previously published values for modern mollusks (Steuber, 1999), brachiopods (Brand et al., 2003; Delaney et al., 1989; Ullmann et al., 2017) and sea urchins (Carpenter and Lohmann, 1992; LaVigne et al., 2013).

The Li/Ca ratios of bivalve mollusk from this study range between 3.7 to 52.0 μmol.mol^{-1}, while the only gastropod, *Turritella*, has the lowest Li/Ca value (1.7 μmol.mol^{-1}) of all the samples. Brachiopods have Li/Ca ratios ranging from 20 to 43 μmol.mol^{-1}, while the high-Mg calcite echinoderm specimens have the highest Li/Ca of this dataset, ranging from 60 to 81 μmol.mol^{-1}. The Li/Ca of our samples are within the range of previously published Li/Ca from the literature (see Fig. 4). If we consider all reported measurements (including measurements made at various parts on a single shell), the range of Li/Ca ratio of biogenic calcite is very high with values up to 250 μmol.mol^{-1} measured on some part of the Bivalve *Pecten maximus* (Thébault and Chauvaud, 2013). However, if we consider only the average value for each specimen, Li/Ca ratio ranges from 10 to 50 μmol.mol^{-1} for LMC organisms, between 1 and 30 μmol.mol^{-1}.for aragonitic speciments, and between 60 and 90 μmol.mol^{-1} for High-Mg calcite biogenic carbonates, showing that there is a mineralogical control on the Li/Ca of biogenic carbonate (Fig. 4b). Furthermore, there is an overall correlation between Li/Ca and Mg/Ca (Fig. 3) for all biogenic carbonates, suggesting that these two elements are impacted by one or more common processes during biomineralization.

The elemental compositions of cultured experiment samples (for which the mineralogy was not measured) are in agreement with other samples and plot inside the field defined by each polymorph mineral (Fig. 4). For the oyster sample from List Tidal Basin (assumed to be pure calcite), we observe that 3 samples have much higher Sr/Ca ratio and lower Li/Ca than surrounding samples and plot well outside the trend defined by the mixture between aragonite and calcite. Whether these samples contain some aragonite or high-Mg calcite, or perhaps have been altered, has not be determined. In the absence of additional information, these samples will not be further considered in our interpretation.

4.3. Lithium isotopes

For the entire dataset (Table 1), the Li isotope composition ranges between +14.9 and +40.7‰, indicating that these biogenic carbonates have both lower and higher δ^7Li compared to modern seawater (+31‰). For the modern biogenic carbonates, the pure aragonitic mollusks have the lowest δ^7Li values, ranging from +14.9 to +21.7‰, whereas the pure calcitic mollusks have higher δ^7Li, ranging from +20.5 to +40.7‰ (Fig. 4). Mixed aragonite-calcite samples have intermediate values. For the extensively micro-sampled North Sea oyster sample, the δ^7Li ranges from 20.5 to 37.8‰ with no significant systematic differences between the chalky and foliate layers. The 8 brachiopod and 3 echinoderm samples have

relatively uniform δ^7Li, ranging respectively from +24.7 to +27.8‰ and from +24.1 to +24.4‰ (Fig. 4). The field collected specimens from this study come from various locations that span a wide range of ocean temperatures (–1 to 30°C). As discussed before, because the location of most of the samples is not known precisely, and because natural temperatures may vary seasonally, we assign a 2°C uncertainty to estimated growth temperatures and only look to identify any large first order relationships. We find no effect of temperature on the measured δ^7Li using this approach (Fig. 5B). This lack of correlation is particularly clear for the four specimens of *Crassostrea gigas*, with temperatures ranging from +10 to +22°C (points labelled C.G.1 to C.G.4 in Fig. 5B). In addition, we can also consider the influence of short timescale (weekly to monthly) temperature variation on the Li isotope composition of *Crassostrea gigas* specimen from the North Sea. For this specimen, we establish time series along foliate structure and chalky using growth strata, and calcification temperatures were calculated using the δ^{18}O of each sample (Ullmann et al., 2013a, 2010). No correlation was observed between the calcification temperature and δ^7Li for either the chalky substance or foliate layers, despite the large range of δ^7Li values.

For the samples from growth experiments at various temperatures, the δ^7Li ranges from +32.1 to +35.2‰ from *Pecten maximus* samples, from +33.3 to +39.7‰ for *Mytilus edulis*, and from +17.2 to +19.2‰ for *Mercenaria mercenaria*. Experimental temperatures ranged from 10 to 22°C for the calcitic bivalve mollusks and from 15 to 30°C for the aragonitic bivalves. For the two calcitic calcifiers (*Mytilus edulis* and *Pecten maximus*), we observe a weak positive correlation between measured δ^7Li and temperature for the studied range (r^2=0.3; Fig. 5a). The Li isotope composition is slightly higher at high temperature than at lower temperature with a δ^7Li-temperature relationship of about +0.2‰/°C. For the aragonitic bivalve (*Mercenaria mercenaria*), the opposite relation is observed, with slightly higher δ^7Li at low temperature than at to high temperature (δ^7Li-temperature relationship of –0.1‰/°C).

5. DISCUSSION

The δ^7Li range for biogenic carbonates from this study (+14.9 to +40.7‰) is much larger that the range of previously-reported Li isotope compositions for both inorganic carbonates and modern seawater (Marriott et al., 2004a, 2004b; Misra and Froelich, 2012). This suggests an environmental and/or biological control on the Li isotope composition of

these biogenic carbonates. In this discussion, we explore the influence of mineralogy, temperature, and biology (taxonomic differences, inter-species, and intra-specimen variability) on the Li isotope fractionation of mollusks, brachiopods and sea urchins. We show that biological processes significantly influence the Li isotope composition and Li/Ca ratio of mollusk shells, but not the compositions of the secondary layer (the only one measured in this study) of brachiopods.

5.1. Influence of mineralogy

Experimental inorganic calcium carbonate precipitates have lower δ^7Li values compared to the solution from which they precipitate (Marriott et al., 2004a,b; Gabitov et al., 2011), with aragonite more fractionated ($\Delta^7Li_{aragonite\text{-}solution}$ = –7 to –12‰) than calcite ($\Delta^7Li_{calcite\text{-}solution}$ = –2 to –5‰). Biogenic carbonates also are fractionated differently according to their mineralogy with δ^7Li of calcite shells (excluding samples "ofl04, 05 and 06") from +25 to +40‰ whereas aragonitic shells have δ^7Li from +15 to +24‰ (Fig. 4a), with bi-mineralic shells exhibiting intermediate δ^7Li. These observations are consistent with other types of biogenic carbonates. as the δ^7Li of modern calcitic planktic foraminifera is systematically higher than 26‰ (Hathorne and James, 2006; Misra and Froelich, 2009) whereas corals (aragonite) have δ^7Li consistently lower than +25‰ (Rollion-Bard et al., 2009). Interestingly, the three high-Mg calcite samples (echinoderms) of this study have an intermediate δ^7Li of +24‰. We also note systematic differences in Li/Ca ratio amongst aragonite, calcite and high-Mg calcite samples. The inorganic partition coefficient for Li (relative to Ca) between inorganic carbonates and solution (referred here as Kd^{Li}), determined in abiogenic experiments, is slightly higher for aragonite compared to calcite (Marriott et al., 2004a,b). However, the Li/Ca ratio of aragonitic skeletons is generally lower than biogenic calcite (see the compilation by Hathorne et al., 2013) and this difference is confirmed by this study (Fig. 4b).

The reasons for the differential incorporation of Li and its isotopes between the various inorganic carbonate minerals are not clear. Previous studies have proposed that Li^+ substitutes for the Ca^{2+} site in aragonite, whereas in calcite, Li is incorporated interstitially (Marriott et al., 2004a,b). The larger isotope fractionation observed in inorganic aragonite compared to calcite could be due to the fact that there is less fractionation of Li isotopes during incorporation in the interstitial position in calcite compared to substitution Li^+ for Ca^{2+} in aragonite (Okumura and Kitano, 1986; Tomascak et al., 2016). Additionally, because of

their similar ionic radii, Li often substitutes for Mg in silicate minerals (Tomascak et al., 2016). Hence, differences in Mg binding environment between calcite and aragonite could also potentially explain the different Li isotope composition between these minerals.

5.2. Influence of temperature

The three bivalve species (*Pecten maximus, Mytilus edulis and Mercenaria mercenaria*) grown at different temperatures, keeping other parameters constant, show only weak correlation (r^2 = 0.3 to 0.5) with temperature (Fig. 5a). The δ^7Li of field-collected specimens from various locations show no relationship with temperature. Collectively, these data indicate that temperature has minor influences on δ^7Li within mollusk species but is not the first order control on δ^7Li variability across the mollusk species investigated in this study. This conclusion is consistent with results from inorganic carbonate precipitation experiments (see Fig. 5a) that show no temperature-dependence of carbonate δ^7Li (Marriott et al., 2004a). The same observation was made for experimentally-grown foraminifera *Amphistegina lessonnii* (Vigier et al., 2015). We note that the field-collected coral samples also showed no correlation between temperature and δ^7Li (Marriott et al., 2004a; Rollion-Bard et al., 2009).

In contrast to δ^7Li values, relationships between carbonate Li/Mg, and to a lesser extent Li/Ca, and temperature have been reported in other studies (Marriott et al., 2004a; Montagna et al., 2014; Case et al., 2010; Bryan and Marchitto 2008; Fowell et al., 2016; Hathorne et al., 2013). For inorganic calcite (Marriott et al., 2004a) and brachiopods (Delaney et al., 1989), Li/Ca ratios exhibit a negative relationship with temperature. For corals and foraminifera, very good correlations have been observed between temperature and Li/Mg ratio, suggesting that the latter might be a promising proxy for reconstructing past ocean temperature. We observe that although some samples from this study plot close to the inorganic trend, most samples have higher Li/Ca than inorganic carbonate for a given temperature (not shown). Similar to the case for Li isotopes, temperature does not seem to be the first-order control on Li/Ca of mollusks across species, although it does influence Li/Ca within mollusk species. On the other hand, the brachiopods from this study plot on the same Li/Ca vs. temperature regression as the brachiopods from Delaney et al., (1989) confirming the temperature control of Li/Ca for brachiopods (Fig. 5c).

Considering the relationship between the Li/Mg ratio in mollusks and water temperature, several observations can be made. First, for the growth experiments, for which the temperature has been monitored, we observe a strong correlation between Li/Mg and T

for the species *Mytilus edulis* (r^2 = 0.83; Fig 5D) but no correlation for *Pecten maximus* and *Mercenaria mercenaria*. This is the first time that a correlation between the Li/Mg in a marine bivalve and temperature is reported. This suggests that the Li/Mg ratio in *Mytilus edulis* has great potential for paleo-temperature reconstruction in the ocean. However, more data testing the influence of other parameters are necessary to definitely validate such a calibration. Secondly, the relationship between Li/Mg and T for *Mytilus edulis* is different from the relationships defined by other organisms (e.g. Montagna et al., 2014; Case et al., 2010; Bryan and Marchitto 2008; Fowell et al., 2016), indicating that the relationship between Li/Mg and temperature is taxon-dependent. Finally, if we report also field-collected organisms on the Li/Mg temperature plot (see figure in supplementary materials), we observe that although there is a global trend of decreasing Li/Mg with temperature, the correlation between these two parameters is highly scattered. Thus, contrary to corals, the relationship between Li/Mg and temperature is overall quite weak and therefore it appears difficult to use mollusk Li/Mg to estimate water temperature unless targeting specific species (like *Mytilus edulis).*

5.3. Intra-shell variability

A large intra-shell Li isotope variability (up to 25‰) is observed for bi-mineralic mollusk shells. This is best exemplified by *Mytilus californianus*, for which the inner aragonitic nacreous layer has a δ^7Li as low as 15‰, while the δ^7Li of the outer calcite prismatic layer is about 40‰. All *Mytilus californianus* samples plot on the same negative regression between δ^7Li and the proportion of aragonite measured by XRD (Fig. 6). Interestingly, no variation is observed across the horizontal length of the outer layer (rectangles in Fig. 6). This result indicates that the Li isotope composition of the calcite part of the shell of *Mytilus californianus* is relatively homogenous and independent of shell growth rate or age. In contrast, for the *Chione* shells, dominantly composed of aragonite with a small proportion of calcite (in general < 20%, one sample at 55%), the observed intra-shell variability is much lower (less than 3‰), although the samples with the highest proportion of calcite have systematically highest δ^7Li for each species.

Intra-shell variability was also investigated on a calcitic oyster (*Crassostrea gigas*) and aragonitic clam (*Tridacna maxima*). The observed intra-shell variability of the aragonitic clam is small, less than 2‰ between the outer and inner layer. In contrast, relatively large δ^7Li variability (about 12‰; excluding the anomalous Mg/Ca and Sr/Ca samples) was

observed for *Crassostrea gigas* in at least 3 specimens. However, no significant differences were noticed between the chalky and foliate layers, indicating that Li isotope variability in this oyster is not controlled by the chalky vs. foliate nature of the calcite shell. Finally, intra-shell variability was also tested for a brachiopod shell (*Terebratulina transversa*), for which we observe a limited variability of 2.5‰ between anterior and posterior valves. However, we did not attempt to determine whether the secondary and primary layers of brachiopod shells have similar δ^7Li, as has been done for others isotope proxies (Auclair et al., 2003; Cusack et al., 2012; Parkinson et al., 2005; Penman et al., 2013; Ullmann et al., 2017), and this question remains to be investigated.

In summary, there is significant but not systematic intra-shell variability for some skeletons. The largest intra-shell δ^7Li variability (> 25‰) is controlled by mineralogical mixing between calcite and aragonite, but up to 12‰ variability is also observed in some mineralogically pure species (e.g., the oyster *C. gigas*) while intra-shell variability of less than 2.5‰ is observed in other taxa (*Chione, Tridacna, Terebratulina*).

5.4. Influence of biological processes

5.4.1. Evidence for vital effects

Here, we compare our biogenic samples to inorganic carbonates. Precipitation experiments have shown that the carbonate phase is enriched in ^{6}Li compared to the fluid from which it precipitates (Marriott et al., 2004a,b). Following Planchon et al. (2013), we can define the deviation from inorganic values as $\Delta^7Li_{physiol} = \delta^7Li_{carbonate\ biogenic} - \delta^7Li_{carbonate\ inorganic}$ with "$\delta^7Li_{carbonate\ inorganic}$" being the δ^7Li value of the corresponding inorganic carbonate precipitated from modern seawater ($\delta^7Li_{seawater}$ = 31‰), as derived from the experiments by Marriott et al. (2004a,b). We use a $\Delta^7Li_{calcite\text{-}solution}$ value of –3‰ for the δ^7Li of inorganic calcite and a $\Delta^7Li_{aragonite\text{-}solution}$ value of –12‰ for inorganic aragonite (Marriott et al., 2004b, 2004a). The $\Delta^7Li_{physiol}$ values of mollusk shells range from –4 to +14‰ (Fig. 7). This suggests a strong vital effect on the incorporation of Li isotopes in mollusk shells. The $\Delta^7Li_{physiol}$ of brachiopods ranges between 0 and –3‰ (average of –1.4‰, n = 8 measurements), suggesting a limited influence of vital effects for this group of organisms. Interestingly, the $\Delta^7Li_{physiol}$ values are larger and more positive for calcitic mollusk shells (i.e. they preferentially incorporate the heavy isotope ^{7}Li) compared to aragonitic shells. This result indicates that physiological processes favor the utilization of the light isotope for aragonitic mollusks and the heavy isotope for calcitic mollusks. The influence of vital effects

on Li isotope composition have also been identified for benthic foraminifera by Vigier et al. (2015) who showed that the δ^7Li of cultured *Amphistegina* benthic foraminifera can be as low as 21‰ and as high as 38‰, depending upon the DIC concentration of seawater.

Regarding the Li/Ca values, as observed by Hathorne et al. (2013) and described in section 5.2., biogenic calcite has higher average Li/Ca than biogenic aragonite, the opposite of what is observed for inorganic carbonates (Marriott et al., 2004a,b). This apparent conundrum may be explained by the influence of physiological processes that either favor Li incorporation for calcite relative to aragonite through the involvement of specific cellular processes or if there is a strong influence of the pH and/or calcification rate (as suggested by the study of Gabitov et al., 2011) on the inorganic equilibrium partition coefficients. This stresses the need for more experiments looking at the controls on the inorganic partition coefficients and specifically the role of pH and calcification rates.

In order to remove variability arising from differences between partition coefficient of inorganic calcite and aragonite, we normalize the observed partition coefficient of Li between biogenic carbonate and seawater [D^{Li} = $(Li/Ca)_{biogenic\ carb.}$ / $(Li/Ca)_{seawater}$] to the partition coefficient between inorganic carbonates and seawater [Kd^{Li} = $(Li/Ca)_{inorganic\ carb.}$ / $(Li/Ca)_{seawater}$]. We define this parameter as $\beta^{Li} = D^{Li}/Kd^{Li}$ to express the enrichment or depletion in Li (relative to Ca) in the biogenic carbonate relative to inorganic carbonate, i.e., the enrichment or depletion in Li in shells due to physiological processes only. As discussed previously, inorganic experiments have shown that Kd^{Li} (defined as "D^{Li}" in Marriott et al., 2004 but referred to here as "Kd^{Li}") for calcite is a function of temperature. Hence for each sample, the β^{Li} value should be calculated with the Kd^{Li} corresponding to the growing temperature of the shell. However, as discussed before, there is a large uncertainty on the growth temperature of field-collected shells from this study. In addition, the relationship between Kd^{Li} and temperature for aragonite has yet to be experimentally investigated. Therefore, we consider both (i) β^{Li} values normalized to the Kd^{Li} determined at 25°C, which we will refer to as "$\beta^{Li}{}_{25°C}$" and (ii) $\beta^{Li}{}_{T}$ calculated with the Kd^{Li} value corresponding to the associated growth temperature and applied to aragonite using the same relationship to temperature as determined for calcite. Considering the data from both this study and from the literature (on other biogenic carbonates), the calculated β^{Li} values are between 0.2 and 3 for aragonite skeletons and between 2 and more than 10 for calcite skeletons (Fig. 7). Hence, calcite organisms are systematically enriched in Li relative to inorganic calcite, lilely as a result of Biologically-controlled processes.

5.4.2. Taxonomic differences in δ^7Li and Li/Ca

Comparison of our results with published data reveals important differences in the δ^7Li and Li/Ca ratios between various species, genera and phyla. At the phylum level, the largest differences in Li isotope composition are observed within the group of calcite organisms for which each phylum has a specific pair of $\Delta^7Li_{physiol}$ and β^{Li} values (Fig. 7). The range of $\Delta^7Li_{physiol}$ of modern field-collected calcitic mollusks (–2 to +13‰) is significantly larger compared to modern planktic foraminifera (–2 to +4‰), brachiopods (–3 to 0‰), and benthic foraminifera (–7 to –1‰). Aragonitic calcifiers, including corals (Δ^7Li_{physio} = 0 to +4‰), and aragonitic bivalves (–4 to +1‰), have a smaller range of $\Delta^7Li_{physiol}$. We also observe that for a given $\Delta^7Li_{physiol}$ value, sea urchins, brachiopods, and mollusks have the highest β^{Li}, followed by planktic and benthic foraminifera, followed by aragonite calcifiers. This shows that physiological processes significantly influence the proportion of Li incorporated into the shell of various types of calcifiers.

In addition, we also investigated the importance of inter-genera and inter-species variability by comparing the δ^7Li of shells from various species grown in similar thermal environments. Our dataset reveals large inter-species differences in Li isotope composition of mollusk shells (for a given mineralogy), in contrast to foraminifera and brachiopods. Shells of mollusk species *Mytilus edulis* and *Pecten maximus*, grown at various temperature, all other parameters constant, exhibit systematic Li isotope differences of 4 to 5‰ for seawater temperatures ranging from 10 to 20°C (Fig. 5B). Furthermore, we observe that the two species of *Chlamys* have higher δ^7Li compared to species of other mollusk genera grown at similar temperature. Up to 7‰ variability between species of equivalent mineralogy is observed at a given temperature (Fig. 5B).

5.4.3. Origin of the vital effect for calcite mollusks

When $\Delta^7Li_{physiol}$ values are compared to $\beta^{Li}{}_{25°C}$ for mollusks (Fig.7), we observe a negative correlation between $\Delta^7Li_{physiol}$ and $\beta^{Li}{}_{25°C}$ for *Mytilus edulis* specimens grown at various temperature (r^2=0.85). Interestingly, this relationship is also observed for all calcitic mollusks (r^2=0.63) from this study. For the temperature-normalized inorganic Li/Ca ratios ($\beta^{Li}{}_T$), the correlation is less good but still holds for calcite mollusks (r^2=0.45) but not for *Mytilus edulis* specimens (r^2=0.21). For aragonite mollusks, we also observe a negative correlation between $\Delta^7Li_{physiol}$ and $\beta^{Li}{}_{25°C}$ (r^2=0.47) but no correlation is observed with $\beta^{Li}{}_T$. In

this section, we discuss several hypotheses for explaining this correlation and relate these observations to potential mechanisms of Li isotope fractionation during biomineralization.

Most skeletal organisms calcify in a reservoir isolated from external seawater. They favor calcification by either (i) increasing saturation state (by increasing their internal pH, DIC and/or internal Ca concentration), (ii) reducing their internal fluid Mg/Ca ratio (in particular for modern calcite organisms), or (iii) using a complex organic template to control orientation and distribution of crystals during nucleation (Immenhauser et al., 2016; Ries, 2010). These pathways are not mutually exclusive. Mollusks have an extracellular-type process of biomineralization (Immenhauser et al., 2016; Weiner and Addadi, 2011; Weiner and Dove, 2003). Precipitation of the inner layer is inferred to take place somewhere in the extrapallial space (which contains extrapallial fluid or EPF), located between the inner shell surface and the outer mantle epithelium. For the outer layer, the EPF is located between the prismatic layer and the mantle epithelium. The EPF contains inorganic ions and various organic molecules that interact to form the biominerals. Precipitation is controlled by specialized cells of the outer mantle epithelium that release complex organic macromolecules that are used as organic templates for controlling the morphology of precipitated crystals. Usually, a precursor amorphous carbonate phase (ACC) is first precipitated and then transformed to calcite or aragonite (Baronnet et al., 2008, Weiner and Addadi, 2011). It has been suggested that precursor amorphous phases are also used by echinoderms (Beniash et al., 1997).

The negative relationship between $\Delta^7Li_{physiol}$ and β^{Li} for calcite mollusks cannot be produced by carbonate precipitation alone (e.g., by varying proportions of Li incorporated into carbonates) because (i) the partitioning of Li between the carbonates and the fluid strongly favors the fluid ($Kd^{Li}<<1$), hence very small amount of Li is incorporated into carbonate minerals and therefore carbonate precipitation does not change the δ^7Li of the fluid and (ii) carbonates would have δ^7Li lower than seawater, not higher as observed for most of the mollusk samples, because ^{6}Li is preferentially incorporated into inorganic carbonates. Furthermore, it has been argued that in bivalves, passive ion transport through ion channels to the calcification site results in similar composition in the extrapallial space as in the seawater (Immenhauser et al., 2016). Hence, the most likely explanation for the observed trends is that the δ^7Li and Li concentration of the calcification fluid is modified prior to carbonate precipitation by physiological processes leading to addition or removal of Li in the internal calcification medium and that this process also fractionates Li isotopes.

This type of mechanism was recently proposed by Vigier et al. (2015) for explaining the range of Li/Ca and δ^7Li of cultured foraminifera of the genus *Amphistegina* at low and high DIC concentrations. In this conceptual model, elevation of pH within the seawater vacuoles is achieved by a Na/proton exchanger that removes protons from the vacuoles and transports Na (and Li) inside the vacuoles (Bentov et al., 2009; Erez, 2003). These vacuoles are then transported into the calcification site of foraminifera where the organic matrix is present (Bentov et al., 2009; Erez, 2003). At low DIC concentration, the activity of the Na/proton exchanger would be more intense and more Li would be transported into the calcification site (Vigier et al., 2015). Assuming this process fractionates Li isotopes (for example by kinetic or enzymatic isotope fractionation), the result would be an increase in the Li/Ca ratio and a decrease in the δ^7Li of the calcification reservoir relative to seawater (i.e. negative $\Delta^7Li_{physiol}$ values). This is what we observe for aragonite mollusks as most of the samples have negative $\Delta^7Li_{physiol}$ values. Moreover, benthic foraminifera and some calcite mollusks and brachiopods also have slightly negative $\Delta^7Li_{physiol}$ values (Fig. 7). Hence, this process could potentially explain their variability in Li isotope and Li/Ca ratios. However, the great majority of calcitic mollusks and foraminifera have positive $\Delta^7Li_{physiol}$ values, which implies the need for a different explanation.

Another possibility, is that Li is actively removed from the calcification site, with an isotope fractionation leading to preferential removal of ^{6}Li (Vigier et al., 2015). This process would lead to high δ^7Li (high $\Delta^7Li_{physiol}$) and low Li/Ca (low β^{Li}) of carbonates. Removal of Mg from the calcification reservoir through Mg specific channels has previously been suggested for foraminifera (Bentov and Erez, 2006; Zeebe and Sanyal, 2002) to explain their low Mg/Ca value relative to seawater, even if the relevance of this process is debated (Pogge von Strandmann et al., 2014; Wombacher et al., 2011). Indeed, high Mg content in fluids inhibits calcite precipitation (e.g. Berner, 1975), so removal of Mg is one possible strategy to favor calcite precipitation (Ries, 2010; Wang et al., 2013; Bentov and Erez, 2006; Zeebe and Sanyal, 2002). As Li is often associated with Mg, we suggest that similarly to Mg, Li could be transported out of the calcification site by specific channels and/or pumps (Bentov and Erez, 2006). This hypothesis is supported by the negative correlation between δ^7Li and Mg/Ca for calcitic mollusks (Fig. 8B), indicating that, indeed, mollusks having the highest δ^7Li also have the lowest Mg/Ca ratio.

The process of Li removal from the calcification site can be modeled in a simple way as either (i) an open system at steady-state (input fluxes are balanced by output fluxes) or (ii) a

closed or semi-enclosed system, corresponding to non-steady-state conditions with output fluxes being higher than input fluxes (requiring periodic 'batch' replenishment of the calcifying medium). For the latter, the Li/Ca and Li isotope composition of the fluid inside the calcification reservoir evolves following a Rayleigh distillation as a function of the proportion of Ca and Li removed.

The corresponding equation for the open system at steady-state is:

and for the closed system:

$$\Delta_{physiol} = \Delta_{pump-fluid} \times \ln(\gamma_{fluid}^{Li}) \quad (2)$$

with $\Delta^7Li_{pump\text{-}fluid}$ being the fractionation factor ($\Delta^7Li_{pump\text{-}fluid}$ = 1000 ln($\alpha_{pump\text{-}fluid}$)) between the Li removed and the Li within the calcification site, and γ_{fluid}^{Li} being the proportion of Li remaining in the fluid in the calcification reservoir after Li extrusion, calculated as the ratio between the concentration of Li remaining in the reservoir after extrusion divided by the initial concentration of Li before extrusion. Assuming that there is no Ca removal by this process, then we can express γ_{fluid}^{Li} as:

$$\gamma_{fluid}^{Li} = \frac{(Li/Ca)_{fluid}}{(Li/Ca)_0} = \frac{(Li/Ca)_{carb}}{(Li/Ca)_{carb-0}} = \frac{\beta^{Li}}{\beta_0^{Li}} \quad (3)$$

With the subscript "fluid" corresponding to the fluid in the calcification reservoir, "0" to initial fluid in the calcification reservoir before Li removal, "carb" to carbonate and "carb-0" to the composition of the carbonate formed in the absence of Li extrusion (i.e. when $(Li/Ca)_{res} = (Li/Ca)_0$). Hence, equations 1 and 2 can be combined to give:

$$\Delta_{physiol} = -\Delta_{pump-fluid} \times \left(1 - \frac{\beta^{Li}}{\beta_0^{Li}}\right) \quad (4)$$

$$\Delta_{physiol} = \Delta_{pump-fluid} \times \ln\left(\frac{\beta^{Li}}{\beta_0^{Li}}\right) \quad (5)$$

The $\Delta^7Li_{physiol}$ and $\beta^{Li}{}_{25°C}$ data for calcite mollusks can be fitted by equations (4) and (5) assuming that (i) all the mollusks have a relatively similar initial β_0^{Li} at the calcification site and (ii) there is unique associated isotope fractionation factor ($\Delta^7Li_{pump\text{-}fluid}$) for all mollusks. The best fits (both giving r^2 = 0.64) corresponding to both the closed and open system isotope fractionation for calcite mollusks are represented on Fig. (8). The trends intercept the grey line corresponding to the absence of vital effects ($\Delta^7Li_{physiol}$ = 0) at a $\beta_{25°C}^{Li}$

value of 7±1 for the open system and at 7.5±1.0 for the closed system (Fig. 8A). Hence, the initial Li/Ca ratio of the mollusks, in the absence of Li extrusion, is about 7 times higher than the Li/Ca ratio of inorganic calcite. Investigation of the reasons for such high $\beta^{Li}_{25°C}$ values for mollusks is beyond the scope of this study but preferential incorporation of Ca in carbonates (e.g., Elderfield et al., 1996) and/or specific Ca input or removal from the calcification site through channel pump or exchange enzyme transporter (Carré et al., 2006) could potentially explain $\beta^{Li}_{25°C}$ higher than 1. Regarding the fractionation factor, we obtain a $\Delta^7Li_{pump\text{-}fluid}$ value of –15‰ ($\alpha_{pump\text{-}fluid}$ = 0.985) for the open system and –9‰ ($\alpha_{pump\text{-}fluid}$ = 0.991) for the closed system model. We hypothesize that this fractionation corresponds to a kinetic isotope fractionation where the ^{6}Li is preferentially extruded from the calcification site by diffusion or active transport through membranes. For diffusion in water at low temperature, the Li isotope fractionation is relatively small (about 0.997; Richter et al., 2006) whereas the fractionation factor through a membrane at 22°C was determined to be 0.989 by Fritz (1992). The latter value is close to the fractionation factor corresponding to closed system (Rayleigh) fractionation inferred in our model. As represented in Fig. (8), we calculate that up to 80% of the Li initially present at the calcification site is removed before precipitation of calcite for mollusks. We note that this mechanism could also explain the high $\Delta^7Li_{physiol}$ and low $\beta^{Li}{}_{25°C}$ values of *Amphistegina* benthic foraminifera growth at high DIC concentration from Vigier et al. (2015). Indeed, we can speculate that in foraminifera both addition of Li (through the Na^+/H^+ transporter) and removal of Li (coincident with Mg removal) exist. At high DIC concentration, the activity of the Na^+/H^+ transporter (leading to low $\Delta^7Li_{physiol}$) is lowered, so removal of Li becomes dominant with resulting $\Delta^7Li_{physiol}$ value being higher. Ultimately, the Li isotope composition of biogenic carbonates is probably controlled by the balance between processes removing and adding dissolved Li to the calcification medium.

6. Implications for reconstructing past seawater composition

One goal of this study is to test whether and how different biocalcifying organisms may be used to reconstruct the past δ^7Li of seawater. The secondary layers of brachiopods analyzed here have homogeneous δ^7Li, with little apparent influence from vital effects, temperature, and inter-species differences. In addition, as previously observed by Delaney et al. (1989), the Li/Ca of brachiopods may be a reliable proxy for tracing past ocean temperature if Li/Ca of the ocean is known or, conversely, determining past Li/Ca of the ocean if the calcification temperature is known through other proxies. Collectively, these

observations suggest that brachiopods are promising candidates as archives of past Li isotope composition of seawater. However, as we only analyzed 5 different specimens from 5 different species, we suggest caution in interpreting these results and urge more analyses of present-day brachiopods (including considering intra-shell variability) to confirm these conclusions.

Unlike brachiopods, the range of δ^7Li and Li/Ca values of modern calcitic mollusks is large and significantly influenced by physiological processes, inter-species and inter-specimen differences. Therefore, fossil shells of calcitic mollusks are probably not good targets for inferring the past Li isotope composition or temperature of the oceans, unless the reconstructions are limited to single species. As mollusks can constitute a significant component of bulk carbonates (Wilkinson, 1979), it is important to take them into account to understand the Li isotope composition of bulk carbonates (Lechler et al., 2015; Pogge von Strandmann et al., 2013), at least when these are fossiliferous. The δ^7Li and Li/Ca values of aragonitic mollusks are similar to inorganic aragonite composition. Therefore, they are likely to be better archives for marine δ^7Li that calcitic mollusks. However, aragonite mollusks are also more prone to diagenetic transformation and, at this stage, it is not known how diagenesis affects primary δ^7Li signatures. The small subset of echinoderm skeletons analyzed here point to a relatively narrow range of values, but more work would need to be done to establish whether these observations are systematic and the extent to which the signal in high-Mg calcite is preserved during diagenesis.

The results of this study have important implications for the interpretation of Li isotope and Li/Ca data from bulk Phanerozoic carbonates. Over time, the δ^7Li of bulk carbonates is potentially influenced by several parameters including seawater Li isotope composition, mineralogy, diagenesis, the proportion of skeletal to non-skeletal carbonates, taxonomy, temperature of the skeletal carbonates. We have found that different genera have distinct δ^7Li (ranging by several tens of per mil) and distinct Li/Ca ratio, and therefore it is likely that the Li/Ca and Li isotope variability of bulk carbonates can be controlled to some extent by the relative contributions of different taxonomic groups (Fig. 7c). This effect may be most pronounced at times of major change in ecosystem structure, for example, during extinction events. There is also evidence that the overall pattern of biomineralization has significantly changed during Phanerozoic time with an increase in the proportion of skeletal to non-skeletal carbonates over time, together with large changes in the type of skeletal carbonates (Kiessling et al., 2003; Milliman, 1993; Wilkinson, 1979). Additionally, any global change of

the main carbonate mineralogy over time (e.g. calcite and aragonite seas during the Phanerozoic, Stanley and Hardie, 1998) would likely have influenced bulk carbonate δ^7Li because calcite has higher δ^7Li than aragonite for both inorganic and biogenic carbonates. Hence, any long-term reconstruction of past δ^7Li of seawater using bulk carbonates must take into account the influence of secular changes in mineralogy and taxonomic origin of the carbonate that is preserved.

7. Conclusions

In this study, we measured for the first time the Li isotope composition of modern mollusks, brachiopods, and echinoderms in order to test whether these samples are viable targets for determining the past δ^7Li of the ocean and to provide further insight into the geochemistry of biomineralization. We investigated both modern field-collected shells from various environments and shells experimentally grown at various temperatures. We considered the influence of mineralogy, temperature, taxonomy, and vital effects on the Li isotope and Li/Ca composition of biogenic carbonates. The major conclusions are:

1. Brachiopods are promising targets for tracing past Li isotope composition of the ocean because they have similar δ^7Li compared to inorganic calcite precipitated from seawater, (i.e. not significantly affected by vital effects) and exist since the Cambrian, (i.e. available for study in deep time).
2. There is a strong mineralogical control on the δ^7Li of biogenic carbonates. Calcite shells have δ^7Li between +25 to +40‰ while aragonitic organisms have δ^7Li systematically lower than 25‰. High-Mg calcite echinoderm shells have intermediate δ^7Li of +24‰.
3. Only a small influence of temperature is observed in mollusks from growth experiments, and no relation between temperature and δ^7Li is observed for modern field-collected mollusks.
4. There is strong physiological control on the δ^7Li of mollusks. When normalized to inorganic fractionation ($\Delta^7Li_{physiol} = \delta^7Li_{carbonate\ biogenic} - \delta^7Li_{carbonate\ inorganic}$), calcite mollusks display positive and widely ranging $\Delta^7Li_{physiol}$ values, between −1 and +14‰, which indicates influence of physiological effects. Aragonite mollusks exhibit less variability than calcite mollusks, with $\Delta^7Li_{physiol}$ ranging from +1 to –4‰, with most of the values being negative.
5. Different species collected from thermally equivalent vary by up to 7‰ indicating substantial inter-species and inter-genera variability. In addition, intra-shell variability

can be very high for bi-mineralic mollusk shells. Hence, systematically measuring the mineralogy of samples from mineralogical from multi-mineralic shells, is an important pre-requisite for inferring a representative δ^7Li.

6. Interestingly, the Li isotope composition of calcite mollusks is negatively correlated with shell Li/Ca ratio. This is best explained by a simple fractionation model driven by Li removal from the calcification site and an associated single isotope fractionation. We propose that this process is related to combined Mg and Li removal from the calcification site of calcite mollusk in order to lower Mg/Ca of the calcifying medium in support of calcite precipitation.

Acknowledgements:

This work was primarily supported by the American Chemical Society Petroleum Research Fund (award 53418-DNI2 to AJW). We thank the Los Angeles County Museum of Natural History for providing bivalve samples. We thank Jonathan Erez and an anonymous reviewer for their constructive comments on the manuscript. RAE and JBR acknowledge support from NSF grants OCE #1437166 and 1437371. PPvS and CVU analyses of *C. gigas* were funded by NERC Advanced Fellowship NE/I020571/2 and ERC Consolidator grant 682760 - CONTROLPASTCO2.

References:

Angino, E. E., & Billings, G. K. (1966). Lithium content of sea water by atomic absorption spectrometry. Geochimica et Cosmochimica Acta, 30(2), 153-158.

Auclair, A. C., Joachimski, M. M., & Lécuyer, C. (2003). Deciphering kinetic, metabolic and environmental controls on stable isotope fractionations between seawater and the shell of Terebratalia transversa (Brachiopoda). Chemical Geology, 202(1-2), 59-78.

Bagard, M.-L., West, A.J., Newman, K., Basu, A.R., 2015. Lithium isotope fractionation in the Ganges–Brahmaputra floodplain and implications for groundwater impact on seawater isotopic composition. Earth Planet. Sci. Lett. 432, 404–414. doi:10.1016/j.epsl.2015.08.036.

Beniash, E., Aizenberg, J., Addadi, L., & Weiner, S. (1997). Amorphous calcium carbonate transforms into calcite during sea urchin larval spicule growth. *Proceedings of the Royal Society of London B: Biological Sciences*, *264*(1380), 461-465.

Bentov, S., Brownlee, C., & Erez, J. (2009). The role of seawater endocytosis in the biomineralization process in calcareous foraminifera. *Proceedings of the National Academy of Sciences*, *106*(51), 21500-21504.

Bentov, S., & Erez, J. (2006). Impact of biomineralization processes on the Mg content of foraminiferal shells: A biological perspective. *Geochemistry, Geophysics, Geosystems*, *7*(1).

Berner, R. A. (1975). The role of magnesium in the crystal growth of calcite and aragonite from sea water. *Geochimica et Cosmochimica Acta*, *39*(4), 489-504.

Bouchez, J., Blanckenburg, F. von, Schuessler, J.A., 2013. Modeling novel stable isotope ratios in the weathering zone. Am. J. Sci. 313, 267–308. doi:10.2475/04.2013.01.

Brand, U., Logan, A., Hiller, N., & Richardson, J. (2003). Geochemistry of modern brachiopods: applications and implications for oceanography and paleoceanography. *Chemical Geology*, *198*(3-4), 305-334.

Bryan, S.P., Marchitto, T.M., 2008. Mg/Ca-temperature proxy in benthic foraminifera: New calibrations from the Florida Straits and a hypothesis regarding Mg/Li. Paleoceanography 23, n/a-n/a. doi:10.1029/2007PA001553

Carpenter, S.J., Lohmann, K.C., 1992. ratios of modern marine calcite: Empirical indicators of ocean chemistry and precipitation rate. Geochim. Cosmochim. Acta 56, 1837–1849. doi:10.1016/0016-7037(92)90314-9

Carré, M., Bentaleb, I., Bruguier, O., Ordinola, E., Barrett, N.T., Fontugne, M., 2006. Calcification rate influence on trace element concentrations in aragonitic bivalve shells: Evidences and mechanisms. Geochim. Cosmochim. Acta 70, 4906–4920. doi:10.1016/j.gca.2006.07.019.

Carriker, M. R., & Palmer, R. E. (1979). A new mineralized layer in the hinge of the oyster. *Science*, *206*(4419), 691-693.

Carriker, M. R., Palmer, R. E., Sick, L. V., & Johnson, C. C. (1980). Interaction of mineral elements in sea water and shell of oysters (Crassostrea virginica (Gmelin)) cultured in controlled and natural systems. *Journal of experimental marine biology and ecology*, *46*(2), 279-296.

Case, D.H., Robinson, L.F., Auro, M.E., Gagnon, A.C., 2010. Environmental and biological controls on Mg and Li in deep-sea scleractinian corals. Earth Planet. Sci. Lett. 300, 215–225. doi:10.1016/j.epsl.2010.09.029

Chan, L.H., Edmond, J.M., Thompson, G., Gillis, K., 1992. Lithium isotopic composition of submarine basalts: implications for the lithium cycle in the oceans. Earth Planet. Sci. Lett. 108, 151–160. doi:10.1016/0012-821X(92)90067-6

Cusack, M., & Huerta, A. P. (2012). Brachiopods recording seawater temperature—A matter of class or maturation?. Chem. Geol., 334, 139-143.

Darrenougue, N., De Deckker, P., Eggins, S., Payri, C., 2014. Sea-surface temperature reconstruction from trace elements variations of tropical coralline red algae. Quat. Sci. Rev. 93, 34–46. doi:10.1016/j.quascirev.2014.03.005

Delaney, M.L., Popp, B.N., Lepzelter, C.G., Anderson, T.F., 1989. Lithium-to-calcium ratios in Modern, Cenozoic, and Paleozoic articulate brachiopod shells. Paleoceanography 4, 681–691. doi:10.1029/PA004i006p00681

Delaney, M.L., W.H.Bé, A., Boyle, E.A., 1985. Li, Sr, Mg, and Na in foraminiferal calcite shells from laboratory culture, sediment traps, and sediment cores. Geochim. Cosmochim. Acta 49, 1327–1341. doi:10.1016/0016-7037(85)90284-4

Dellinger, M., Gaillardet, J., Bouchez, J., Calmels, D., Louvat, P., Dosseto, A., Gorge, C., Alanoca, L., Maurice, L., 2015. Riverine Li isotope fractionation in the Amazon River basin controlled by the weathering regimes. Geochim. Cosmochim. Acta 164, 71–93. doi:10.1016/j.gca.2015.04.042.

Dellinger, M., Bouchez, J., Gaillardet, J., Faure, L., & Moureau, J. (2017). Tracing weathering regimes using the lithium isotope composition of detrital sediments. *Geology*, *45*(5), 411-414.

Dodd, J.R., 1967. Magnesium and Strontium in Calcareous Skeletons: A Review. J. Paleontol. 41, 1313–1329.

Eagle, R.A., Eiler, J.M., Tripati, A.K., Ries, J.B., Freitas, P.S., Hiebenthal, C., Wanamaker Jr., A.D., Taviani, M., Elliot, M., Marenssi, S., Nakamura, K., Ramirez, P., Roy, K., 2013. The influence of temperature and seawater carbonate saturation state on 13C–18O bond ordering in bivalve mollusks. Biogeosciences 10, 4591–4606. doi:10.5194/bg-10-4591-2013.

Elderfield, H., Bertram, C.J., Erez, J., 1996. A biomineralization model for the incorporation of trace elements into foraminiferal calcium carbonate. Earth Planet. Sci. Lett. 142, 409–423. doi:10.1016/0012-821X(96)00105-7

Erez, J., 2003. The Source of Ions for Biomineralization in Foraminifera and Their Implications for Paleoceanographic Proxies. Rev. Mineral. Geochem. 54, 115–149. doi:10.2113/0540115

Flesch, G. D., Anderson Jr, A. R., & Svec, H. J. (1973). A secondary isotopic standard for 6Li/7Li determinations. *International Journal of Mass Spectrometry and Ion Physics*, *12*(3), 265-272

Fowell, S.E., Sandford, K., Stewart, J. A., Castillo, K.D., Ries, J.B., Foster, G.L., 2016, Intrareef variations in Li/Mg and Sr/Ca sea surface temperature proxies in the Caribbean reef-building coral *Siderastrea siderea*. Paleoceanography 31: PA002968. doi: 10.1002/2016PA002968

Freitas, P. S., Clarke, L. J., Kennedy, H., & Richardson, C. A. (2012). The potential of combined Mg/Ca and δ18O measurements within the shell of the bivalve *Pecten maximus* to estimate seawater δ18O composition. *Chemical Geology*, *291*, 286-293

Freitas, P.S., Clarke, L.J., Kennedy, H., Richardson, C.A., 2009. Ion microprobe assessment of the heterogeneity of Mg/Ca, Sr/Ca and Mn/Ca ratios in *Pecten maximus* and *Mytilus edulis* (bivalvia) shell calcite precipitated at constant temperature. Biogeosciences 6, 1209–1227. doi:10.5194/bg-6-1209-2009

Freitas, P.S., Clarke, L.J., Kennedy, H., Richardson, C.A., Abrantes, F., 2006. Environmental and biological controls on elemental (Mg/Ca, Sr/Ca and Mn/Ca) ratios in shells of the king scallop *Pecten maximus*. Geochim. Cosmochim. Acta 70, 5119–5133. doi:10.1016/j.gca.2006.07.029

Freitas, P.S., Clarke, L.J., Kennedy, H.A., Richardson, C.A., 2008. Inter- and intra-specimen variability masks reliable temperature control on shell Mg/Ca ratios in laboratory- and field-cultured *Mytilus edulis* and

Pecten maximus (bivalvia). Biogeosciences 5, 1245–1258. doi:10.5194/bg-5-1245-2008
Fritz, S. J. (1992). Measuring the ratio of aqueous diffusion coefficients between 6Li+ Cl− and 7Li+ Cr− by osmometry. *Geochimica et Cosmochimica Acta*, *56*(10), 3781-3789
Froelich, F., Misra, 2014. Was the Late Paleocene-Early Eocene Hot Because Earth Was Flat? An Ocean Lithium Isotope View of Mountain Building, Continental Weathering, Carbon Dioxide, and Earth's Cenozoic Clima. Oceanography 27, 36–49. doi:10.5670/oceanog.2014.06
Füllenbach, C.S., Schöne, B.R., Mertz-Kraus, R., 2015. Strontium/lithium ratio in aragonitic shells of Cerastoderma edule (Bivalvia) — A new potential temperature proxy for brackish environments. Chem. Geol. 417, 341–355. doi:10.1016/j.chemgeo.2015.10.030
Gabitov, R.I., Schmitt, A.K., Rosner, M., McKeegan, K.D., Gaetani, G.A., Cohen, A.L., Watson, E.B., Harrison, T.M., 2011. In situ δ7Li, Li/Ca, and Mg/Ca analyses of synthetic aragonites. Geochem. Geophys. Geosystems 12, Q03001. doi:10.1029/2010GC003322
Hall, J.M., Chan, L.-H., 2004. Li/Ca in multiple species of benthic and planktonic foraminifera: thermocline, latitudinal, and glacial-interglacial variation. Geochim. Cosmochim. Acta 68, 529–545. doi:10.1016/S0016-7037(03)00451-4
Hall, J.M., Chan, L.-H., McDonough, W.F., Turekian, K.K., 2005. Determination of the lithium isotopic composition of planktic foraminifera and its application as a paleo-seawater proxy. Mar. Geol., Ocean Chemistry over the Phanerozoic and its links to Geological Processes 217, 255–265. doi:10.1016/j.margeo.2004.11.015
Hathorne, E.C., Felis, T., Suzuki, A., Kawahata, H., Cabioch, G., 2013. Lithium in the aragonite skeletons of massive Porites corals: A new tool to reconstruct tropical sea surface temperatures. Paleoceanography 28, 143–152. doi:10.1029/2012PA002311
Hathorne, E.C., James, R.H., 2006. Temporal record of lithium in seawater: A tracer for silicate weathering? Earth Planet. Sci. Lett. 246, 393–406. doi:10.1016/j.epsl.2006.04.020
Huh, Y., Chan, L.-H., Edmond, J.M., 2001. Lithium isotopes as a probe of weathering processes: Orinoco River. Earth Planet. Sci. Lett. 194, 189–199. doi:10.1016/S0012-821X(01)00523-4
Huh, Y., Chan, L.-H., Zhang, L., Edmond, J.M., 1998. Lithium and its isotopes in major world rivers: implications for weathering and the oceanic budget. Geochim. Cosmochim. Acta 62, 2039–2051. doi:10.1016/S0016-7037(98)00126-4
Immenhauser, A., Schöne, B.R., Hoffmann, R., Niedermayr, A., 2016. Mollusc and brachiopod skeletal hard parts: Intricate archives of their marine environment. Sedimentology 63, 1–59. doi:10.1111/sed.12231
James, R.H., Palmer, M.R., 2000. The lithium isotope composition of international rock standards. Chem. Geol. 166, 319–326. doi:10.1016/S0009-2541(99)00217-X
Kiessling, W., Flügel, E., Golonka, J., 2003. Patterns of Phanerozoic carbonate platform sedimentation. Lethaia 36, 195–225. doi:10.1080/00241160310004648
Kısakűrek, B., James, R.H., Harris, N.B.W., 2005. Li and δ7Li in Himalayan rivers: Proxies for silicate weathering? Earth Planet. Sci. Lett. 237, 387–401. doi:10.1016/j.epsl.2005.07.019
LaVigne, M., Hill, T. M., Sanford, E., Gaylord, B., Russell, A. D., Lenz, E. A., ... & Young, M. K. (2013). The elemental composition of purple sea urchin (Strongylocentrotus purpuratus) calcite and potential effects of pCO2 during early life stages. *Biogeosciences*, *10*(6), 3465.
Lear, C.H., Rosenthal, Y., 2006. Benthic foraminiferal Li/Ca: Insights into Cenozoic seawater carbonate saturation state. Geology 34, 985–988. doi:10.1130/G22792A.1
Lechler, M., Pogge von Strandmann, P.A.E., Jenkyns, H.C., Prosser, G., Parente, M., 2015. Lithium-isotope evidence for enhanced silicate weathering during OAE 1a (Early Aptian Selli event). Earth Planet. Sci. Lett. 432, 210–222. doi:10.1016/j.epsl.2015.09.052
Li, G., West, A.J., 2014. Evolution of Cenozoic seawater lithium isotopes: Coupling of global denudation regime and shifting seawater sinks. Earth Planet. Sci. Lett. 401, 284–293. doi:10.1016/j.epsl.2014.06.011
Marriott, C.S., Henderson, G.M., Belshaw, N.S., Tudhope, A.W., 2004a. Temperature dependence of δ7Li, δ44Ca and Li/Ca during growth of calcium carbonate. Earth Planet. Sci. Lett. 222, 615–624. doi:10.1016/j.epsl.2004.02.031
Marriott, C.S., Henderson, G.M., Crompton, R., Staubwasser, M., Shaw, S., 2004b. Effect of mineralogy, salinity, and temperature on Li/Ca and Li isotope composition of calcium carbonate. Chem. Geol., Lithium Isotope Geochemistry 212, 5–15. doi:10.1016/j.chemgeo.2004.08.002
Milliman, J., Müller, G., Förstner, F., 1974. Recent Sedimentary Carbonates: Part 1 Marine Carbonates. Springer Science & Business Media.
Milliman, J.D., 1993. Production and accumulation of calcium carbonate in the ocean: Budget of a nonsteady state. Glob. Biogeochem. Cycles 7, 927–957. doi:10.1029/93GB02524
Misra, S., Froelich, P.N., 2012. Lithium isotope history of Cenozoic seawater: changes in silicate weathering and reverse weathering. Science 335, 818–823.

Misra, S., Froelich, P.N., 2009. Measurement of lithium isotope ratios by quadrupole-ICP-MS: application to seawater and natural carbonates. J. Anal. At. Spectrom. 24, 1524–1533. doi:10.1039/B907122A

Misra, S., Greaves, M., Owen, R., Kerr, J., Elmore, A.C., Elderfield, H., 2014. Determination of B/Ca of natural carbonates by HR-ICP-MS. Geochem. Geophys. Geosystems 15, 1617–1628. doi:10.1002/2013GC005049

Montagna, P., McCulloch, M., Douville, E., López Correa, M., Trotter, J., Rodolfo-Metalpa, R., Dissard, D., Ferrier-Pagès, C., Frank, N., Freiwald, A., Goldstein, S., Mazzoli, C., Reynaud, S., Rüggeberg, A., Russo, S., Taviani, M., 2014. Li/Mg systematics in scleractinian corals: Calibration of the thermometer. Geochim. Cosmochim. Acta 132, 288–310. doi:10.1016/j.gca.2014.02.005

Okumura, M., Kitano, Y., 1986. Coprecipitation of alkali metal ions with calcium carbonate. Geochim. Cosmochim. Acta 50, 49–58. doi:10.1016/0016-7037(86)90047-5

Olsen, A., Key, R. M., van Heuven, S., Lauvset, S. K., Velo, A., Lin, X., Schirnick, C., Kozyr, A., Tanhua, T., Hoppema, M., Jutterström, S., Steinfeldt, R., Jeansson, E., Ishii, M., Pérez, F. F., and Suzuki, T.: The Global Ocean Data Analysis Project version 2 (GLODAPv2) – an internally consistent data product for the world ocean, Earth Syst. Sci. Data, 8, 297-323, doi:10.5194/essd-8-297-2016, 2016.

Penman, D.E., Hönisch, B., Rasbury, E.T., Hemming, N.G., Spero, H.J., 2013. Boron, carbon, and oxygen isotopic composition of brachiopod shells: Intra-shell variability, controls, and potential as a paleo-pH recorder. Chem. Geol. 340, 32–39. doi:10.1016/j.chemgeo.2012.11.016

Pistiner, J.S., Henderson, G.M., 2003. Lithium-isotope fractionation during continental weathering processes. Earth Planet. Sci. Lett. 214, 327–339. doi:10.1016/S0012-821X(03)00348-0

Planchon, F., Poulain, C., Langlet, D., Paulet, Y.-M., André, L., 2013. Mg-isotopic fractionation in the manila clam (Ruditapes philippinarum): New insights into Mg incorporation pathway and calcification process of bivalves. Geochim. Cosmochim. Acta 121, 374–397. doi:10.1016/j.gca.2013.07.002

Pogge von Strandmann, P.A.E., Desrochers, A., Murphy, M.J., Finlay, A.J., Selby, D., Lenton, T.M., 2017. Global climate stabilisation by chemical weathering during the Hirnantian glaciation. Geochem. Perspect. Lett. 230–237. doi:10.7185/geochemlet.1726

Pogge von Strandmann, P.A.E., Forshaw, J., Schmidt, D.N., 2014. Modern and Cenozoic records of seawater magnesium from foraminiferal Mg isotopes. Biogeosciences 11, 5155–5168. doi:10.5194/bg-11-5155-2014

Pogge von Strandmann, P.A.E., Jenkyns, H.C., Woodfine, R.G., 2013. Lithium isotope evidence for enhanced weathering during Oceanic Anoxic Event 2. Nat. Geosci. 6, 668–672. doi:10.1038/ngeo1875

Pogge von Strandmann, P.A.P., Henderson, G.M., 2015. The Li isotope response to mountain uplift. Geology 43, 67–70.

Richter, F. M., Mendybaev, R. A., Christensen, J. N., Hutcheon, I. D., Williams, R. W., Sturchio, N. C., & Beloso Jr, A. D. (2006). Kinetic isotopic fractionation during diffusion of ionic species in water. *Geochimica et Cosmochimica Acta*, *70*(2), 277-289.

Ries, J.B., Cohen, A.L., McCorkle, D.C., 2009, Marine calcifiers exhibit mixed responses to CO2-induced ocean acidification. Geology 34: 1131-1134.

Ries, J.B., 2010. Review: geological and experimental evidence for secular variation in seawater Mg/Ca (calcite-aragonite seas) and its effects on marine biological calcification. Biogeosciences. Biogeosciences 7. doi:10.5194/bg-7-2795-2010

Ries, J.B., 2011, Skeletal mineralogy in a high-CO2 world. Journal of Experimental Marine Biology and Ecology 403: 54-64.

Rollion-Bard, C., Blamart, D., 2015. Possible controls on Li, Na, and Mg incorporation into aragonite coral skeletons. Chem. Geol. 396, 98–111. doi:10.1016/j.chemgeo.2014.12.011

Rollion-Bard, C., Vigier, N., Meibom, A., Blamart, D., Reynaud, S., Rodolfo-Metalpa, R., Martin, S., Gattuso, J.-P., 2009. Effect of environmental conditions and skeletal ultrastructure on the Li isotopic composition of scleractinian corals. Earth Planet. Sci. Lett. 286, 63–70. doi:10.1016/j.epsl.2009.06.015

Saenger, C., Wang, Z., 2014. Magnesium isotope fractionation in biogenic and abiogenic carbonates: implications for paleoenvironmental proxies. Quat. Sci. Rev. 90, 1–21. doi:10.1016/j.quascirev.2014.01.014

Stanley, S.M., Hardie, L.A., 1998. Hypercalcification: Paleontology links plate tectonics and geochemistry to sedimentology. GSA Today.

Thébault, J., Chauvaud, L., 2013. Li/Ca enrichments in great scallop shells (Pecten maximus) and their relationship with phytoplankton blooms. Palaeogeogr. Palaeoclimatol. Palaeoecol., Unraveling environmental histories from skeletal diaries - advances in sclerochronology 373, 108–122. doi:10.1016/j.palaeo.2011.12.014

Thébault, J., Schöne, B.R., Hallmann, N., Barth, M., Nunn, E.V., 2009. Investigation of Li/Ca variations in aragonitic shells of the ocean quahog Arctica islandica, northeast Iceland. Geochem. Geophys. Geosystems 10, Q12008. doi:10.1029/2009GC002789

Tomascak, P. B., Magna, T., & Dohmen, R. (2016). *Advances in lithium isotope geochemistry* (pp. 119-146). Berlin: Springer.

Ullmann, C.V., Böhm, F., Rickaby, R.E.M., Wiechert, U., Korte, C., 2013a. The Giant Pacific Oyster (Crassostrea gigas) as a modern analog for fossil ostreoids: Isotopic (Ca, O, C) and elemental (Mg/Ca, Sr/Ca, Mn/Ca) proxies. Geochem. Geophys. Geosystems 14, 4109–4120. doi:10.1002/ggge.20257

Ullmann, C.V., Campbell, H.J., Frei, R., Hesselbo, S.P., Pogge von Strandmann, P.A.E., Korte, C., 2013b. Partial diagenetic overprint of Late Jurassic belemnites from New Zealand: Implications for the preservation potential of δ7Li values in calcite fossils. Geochim. Cosmochim. Acta 120, 80–96. doi:10.1016/j.gca.2013.06.029

Ullmann, C.V., Frei, R., Korte, C., Lüter, C., 2017. Element/Ca, C and O isotope ratios in modern brachiopods: Species-specific signals of biomineralization. Chem. Geol. 460, 15–24. doi:10.1016/j.chemgeo.2017.03.034

Ullmann, C.V., Wiechert, U., Korte, C., 2010. Oxygen isotope fluctuations in a modern North Sea oyster (Crassostrea gigas) compared with annual variations in seawater temperature: Implications for palaeoclimate studies. Chem. Geol. 277, 160–166. doi:10.1016/j.chemgeo.2010.07.019

Veizer, J., Ala, D., Azmy, K., Bruckschen, P., Buhl, D., Bruhn, F., Carden, G.A.F., Diener, A., Ebneth, S., Godderis, Y., Jasper, T., Korte, C., Pawellek, F., Podlaha, O.G., Strauss, H., 1999. 87Sr/86Sr, δ13C and δ18O evolution of Phanerozoic seawater. Chem. Geol. 161, 59–88. doi:10.1016/S0009-2541(99)00081-9

Vigier, N., Rollion-Bard, C., Levenson, Y., & Erez, J. (2015). Lithium isotopes in foraminifera shells as a novel proxy for the ocean dissolved inorganic carbon (DIC). *Comptes Rendus Geoscience*, *347*(1), 43-51.

Vigier, N., Rollion-Bard, C., Spezzaferri, S., Brunet, F., 2007. In situ measurements of Li isotopes in foraminifera. Geochem. Geophys. Geosystems 8, Q01003. doi:10.1029/2006GC001432

Wang, D., Hamm, L.M., Giuffre, A.J., Echigo, T., Rimstidt, J.D., Yoreo, J.J.D., Grotzinger, J., Dove, P.M., 2013. Revisiting geochemical controls on patterns of carbonate deposition through the lens of multiple pathways to mineralization. Faraday Discuss. 159, 371–386. doi:10.1039/C2FD20077E

Wanner, C., Sonnenthal, E.L., Liu, X.-M., 2014. Seawater δ7Li: A direct proxy for global CO2 consumption by continental silicate weathering? Chem. Geol. 381, 154–167. doi:10.1016/j.chemgeo.2014.05.005

Wefer, G., Berger, W.H., 1991. Isotope paleontology: growth and composition of extant calcareous species. Mar. Geol., Anoxic Basins and Sapropel Deposition in the Eastern Mediterranean: Past and Present 100, 207–248. doi:10.1016/0025-3227(91)90234-U

Weiner, S., Addadi, L., 2011. Crystallization Pathways in Biomineralization. Annu. Rev. Mater. Res. 41, 21–40. doi:10.1146/annurev-matsci-062910-095803

Weiner, S., Dove, P.M., 2003. An overview of biomineralization processes and the problem of the vital effect. Rev. Mineral. Geochem. 54, 1–29.

Wilkinson, B.H., 1979. Biomineralization, paleoceanography, and the evolution of calcareous marine organisms. Geology 7, 524–527. doi:10.1130/0091-7613(1979)7<524:BPATEO>2.0.CO;2

Wombacher, F., Eisenhauer, A., Böhm, F., Gussone, N., Regenberg, M., Dullo, W.-C., Rüggeberg, A., 2011. Magnesium stable isotope fractionation in marine biogenic calcite and aragonite. Geochim. Cosmochim. Acta 75, 5797–5818. doi:10.1016/j.gca.2011.07.017

Zeebe, R. E., & Sanyal, A. (2002). Comparison of two potential strategies of planktonic foraminifera for house building: Mg2+ or H+ removal?. *Geochimica et Cosmochimica Acta*, *66*(7), 1159-1169.

Table 1: Data for modern field-collected and growth experiment biogenic carbonates from this study.

Sample name	Sample type	Phyllum	Species	Specimen #	Common name	Sampling location	Dominant mineralogy[1]	δ^7Li (‰)	Aragonite (%)	Calcite (%)	Li/Ca (μmol/mol)	Mg/Ca (mmol/mol)	Al/Ca (μmol/mol)	Sr/Ca (mmol/mol)	δ^{18}O (‰)	Growth temperature[2] (°C)	Annual temperature[3] (°C)
Field-collected Mollusk samples																	
57-12	Mixed	Mollusk	*Chlamys cheritata*		Scallops	Alaska (Kachemak Bay) USA	C	39.3	0	100	19.5	5.7	< LD	1.27		9.9	6.74
167501	Mixed	Mollusk	*Chlamys hastata*		Scallops	Newport Beach, CA USA	C	40.7	0	100	11.0	2.9	< LD	1.00		19.6	18.86
53819	Mixed	Mollusk	*Chlamys squamosus*		Scallops	Zamboanga, Philippine Islands	C > A	38.7	30	70	12.1	11.3	< LD	1.22		28.2	28.15
170315	Mixed	Mollusk	*Chione californiensis*		Clams	San Pedro, CA USA	A > C	18.2	79	21	6.8	0.5	< LD	1.30		19.6	18.86
170315	Inner Layer	Mollusk	*Chione californiensis*		Clams	San Pedro, CA USA	A >> C	15.7	94	6						19.6	18.86
170315	Interm Layer	Mollusk	*Chione californiensis*		Clams	San Pedro, CA USA	A	15.5	100	0						19.6	18.86
86-29	Mixed (ext)	Mollusk	*Chione subimbricata*		Clams	Costa Rica (Golfo de Papagayo)	A > C	22.1	84	16	6.1	0.5	< LD	1.39		28.4	27.47
86-29	Outer Layer	Mollusk	*Chione subimbricata*		Clams	Costa Rica (Golfo de Papagayo)	A	21.7	99	1						28.4	27.47
72-84	Mixed	Mollusk	*Chione subrugosa*		Clams	Peru (Puerto Pizzaro)	C = A	24.4	55	46	7.7	0.3	< LD	1.45		25.0	22.15
72-84	Inner Layer	Mollusk	*Chione subrugosa*		Clams	Peru (Puerto Pizzaro)	A	21.9								25.0	22.15
72-84	Outer Layer	Mollusk	*Chione subrugosa*		Clams	Peru (Puerto Pizzaro)	A > C	21.6	88	12						25.0	22.15
50338	Inner Layer	Mollusk	*Tridacna Maxima*		Clams	Guam, Mariana Islands	A >> C	17.6	98	2						28.6	28.63
50338	Outer Layer	Mollusk	*Tridacna Maxima*		Clams	Guam, Mariana Islands	A >> C	19.5	98	2						28.6	28.63
MT1 PNG		Mollusk	*Tridacna Gigas*		Clams	Cocos, Island, Costa Rica	A	19.3	100	0	3.7	0.4	< LD	2.02		28.1	27.56
83-26	Inner Layer	Mollusk	*Mytilus californianus*	1	Mussel	Washington state, USA	A >> C	16.0	98	2	8.7	0.7	< LD	2.38		11.0	
83-26	Outer Layer	Mollusk	*Mytilus californianus*	1	Mussel	Washington state, USA	C = A	28.7	46	54						11.0	
76-39	Front (outer)	Mollusk	*Mytilus californianus*	2	Mussel	Baja Calif, Mexico	C	39.0	0	100	9.9	5.4	< LD	1.15		19.5	16.32
76-39	Mixed Middle	Mollusk	*Mytilus californianus*	2	Mussel	Baja Calif, Mexico	C > A	35.1	9	91	7.0	4.4	< LD	1.14		19.5	16.32
76-39	Mixed Hinge	Mollusk	*Mytilus californianus*	2	Mussel	Baja Calif, Mexico	A > C	27.7	71	29	8.2	1.3	< LD	1.15		19.5	16.32
76-39	Inner Layer	Mollusk	*Mytilus californianus*	2	Mussel	Baja Calif, Mexico	A >> C	14.9	90	10						19.5	16.32
76-39	Outer Layer	Mollusk	*Mytilus californianus*	2	Mussel	Baja Calif, Mexico	C	39.4	0	100						19.5	16.32
AN88	Mixed	Mollusk	*Laternula Elliptica*		Clams	Terra Nova Bay, Antarctica	A	16.3	100	0	9.0	0.7	< LD	2.37		-1.0	-1.34
	Mixed	Mollusk	*Adamussium Colbecki*		Scallop	Ross sea, Edmundson, Antarctica	C	34.6	0	100	12.9	1.0	< LD	1.36		-1.0	-1.34
	Mixed Top	Mollusk	*Turritella*		Gastropod			19.8	100	0	2.0	0.5	< LD	2.05			
	Mixed Back	Mollusk	*Turritella*		Gastropod			19.8	100	0	1.7	0.3	< LD	2.21			
112-72		Mollusk	*Crassostrea gigas*	1	Oyster	Washington state, USA	C	32.9	0	100	25.1	3.1	< LD	0.75		14.0	11
112-72	Inner Layer	Mollusk	*Crassostrea gigas*	1	Oyster	Washington state, USA	C	36.9	0	100						14.0	11
112-72	Outer Layer	Mollusk	*Crassostrea gigas*	1	Oyster	Washington state, USA	C	33.2	0	100						14.0	11
110-50		Mollusk	*Crassostrea gigas*	2	Oyster	Tomales Bay, CA, USA	C	34.0	0	100	16.0	6.9	< LD	0.77		13.0	12
110-50	Outer Layer	Mollusk	*Crassostrea gigas*	2	Oyster	Tomales Bay, CA, USA	C	31.7	0	100						13.0	12
66-117		Mollusk	*Crassostrea gigas*	3	Oyster	Gulf of Guayaquil, Ecuador	C	34.5	0	100	25.4	20.6	< LD	0.60		24.8	23.04
ofl01	foliate layers	Mollusk	*Crassostrea gigas*	4	Oyster	List Tidal Basin Germany	C >> A	29.9			44.4	10.9		1.19	-1.5	18.6*	
ofl02	foliate layers	Mollusk	*Crassostrea gigas*	4	Oyster	List Tidal Basin Germany	C >> A	30.6			30.1	12.3		1.52	-0.7	15.2*	
ofl03	foliate layers	Mollusk	*Crassostrea gigas*	4	Oyster	List Tidal Basin Germany	C >> A	34.3			29.5	7.3		1.12	-1.3	17.7*	
ofl04	foliate layers	Mollusk	*Crassostrea gigas*	4	Oyster	List Tidal Basin Germany	C >> A	23.8			21.4	13.8		2.08	-1.6	19.0*	
ofl05	foliate layers	Mollusk	*Crassostrea gigas*	4	Oyster	List Tidal Basin Germany	C >> A	22.0							-1.4	18.3*	
ofl06	foliate layers	Mollusk	*Crassostrea gigas*	4	Oyster	List Tidal Basin Germany	C >> A	20.5			22.9	7.5		2.58	-0.7	15.2*	
ofl07	foliate layers	Mollusk	*Crassostrea gigas*	4	Oyster	List Tidal Basin Germany	C >> A	26.0			40.9	10.8		0.90	-0.1	12.6*	
ofl08	foliate layers	Mollusk	*Crassostrea gigas*	4	Oyster	List Tidal Basin Germany	C >> A	29.7			29.6	10.4		1.70	0.0	12.2*	
ofl09	foliate layers	Mollusk	*Crassostrea gigas*	4	Oyster	List Tidal Basin Germany	C >> A	34.0			35.9	3.5		1.08	-0.9	16.1*	
ofl10	foliate layers	Mollusk	*Crassostrea gigas*	4	Oyster	List Tidal Basin Germany	C >> A	37.8			32.3	9.1		0.93	-1.8	20.3*	
ofl11	foliate layers	Mollusk	*Crassostrea gigas*	4	Oyster	List Tidal Basin Germany	C >> A	25.5			21.5	8.7		1.44	-1.4	18.2*	
och01	chalky substance	Mollusk	*Crassostrea gigas*	4	Oyster	List Tidal Basin Germany	C >> A	25.6			34.4	14.3		0.87		12.1*	
och02	chalky substance	Mollusk	*Crassostrea gigas*	4	Oyster	List Tidal Basin Germany	C >> A	26.7			30.8	12.4		0.83	-1.1	16.9*	
och03	chalky substance	Mollusk	*Crassostrea gigas*	4	Oyster	List Tidal Basin Germany	C >> A	26.1			31.2	13.9		0.83	-1.6	19.1*	
och04	chalky substance	Mollusk	*Crassostrea gigas*	4	Oyster	List Tidal Basin Germany	C >> A	26.4			34.5	11.0		0.86	-1.9	20.4*	
och05	chalky substance	Mollusk	*Crassostrea gigas*	4	Oyster	List Tidal Basin Germany	C >> A	26.0			24.0	13.3		2.35	-1.6	19.4*	
och06	chalky substance	Mollusk	*Crassostrea gigas*	4	Oyster	List Tidal Basin Germany	C >> A	26.9			35.6	9.1		0.79	-1.7	19.6*	
och07	chalky substance	Mollusk	*Crassostrea gigas*	4	Oyster	List Tidal Basin Germany	C >> A	28.9							-2.0	21.1*	
och08	chalky substance	Mollusk	*Crassostrea gigas*	4	Oyster	List Tidal Basin Germany	C >> A	34.7			52.5	13.4		0.87	-2.1	21.5*	
och09	chalky substance	Mollusk	*Crassostrea gigas*	4	Oyster	List Tidal Basin Germany	C >> A	28.2			43.2	10.7		1.00	-1.4	18.3*	
och10	chalky substance	Mollusk	*Crassostrea gigas*	4	Oyster	List Tidal Basin Germany	C >> A	29.5							-1.4	18.4*	
och11	chalky substance	Mollusk	*Crassostrea gigas*	4	Oyster	List Tidal Basin Germany	C >> A	28.8			42.3	10.6		0.96	-0.7	15.2*	
Field-collected Brachiopod samples																	
	Mixed	Brachiopoda	*Campages mariae*		Brachiopod	Aliguay Island, Philippines	C	26.1			25.9	9.0	< LD	1.12		28.8	28.23
	Mixed	Brachiopoda	*Laqueus Rubellus*		Brachiopod	Sagami Bay, Japan	C	27.8			24.8	4.9	< LD	1.05		18.0	15.87
	Mixed	Brachiopoda	*Terebratulina Transversa*		Brachiopod	Puget Sound, Nr. Friday, Harbor, Washington, USA	C	24.7			29.3	15.4	< LD	1.41		9.0	9.00
	Back-Dorsal	Brachiopoda	*Terebratulina Transversa*		Brachiopod	Puget Sound, Nr. Friday, Harbor, Washington, USA	C	26.7									
	Back-Ventral	Brachiopoda	*Terebratulina Transversa*		Brachiopod	Puget Sound, Nr. Friday, Harbor, Washington, USA	C	26.7									
	Front-Dorsal	Brachiopoda	*Terebratulina Transversa*		Brachiopod	Puget Sound, Nr. Friday, Harbor, Washington, USA	C	27.3									
	Mixed	Brachiopoda	*Notosaria nigricans*		Brachiopod	South Island, New Zealand	C	26.0	0	100	43.0	10.5	< LD	1.41		9.0	9.00
	Mixed	Brachiopoda	*Frenulina sanguinolenta*		Brachiopod	Mactan Island, Philippines	C	27.7			20.1	17.4	< LD	1.27		29.3	29.3
Field-collected Echinoderm samples																	
	Mixed	Sea Urchin	*Strongylocentrotus fransiscanus*		Urchins	Leo Carillo, CA, USA	C	24.4	0	100	69.2	88.2	< LD	2.62		18.6	
	Mixed	Sea Urchin	*Strongylocentrotus purpuratus*		Urchins	Leo Carillo, CA, USA	C	24.1			60.3	80.7	0.064	2.50		18.6	
	Mixed	Sea Urchin	*Dendraster*		Urchins	Morro Bay, CA, USA	C	24.2	0	100	81.3	109.1	0.086	2.4		14.7	
Growth experiment mollusks samples																	
15A2 Nac		Mollusk	*Mercenaria Mercenaria*	1	Clams	Growth experiment	A >> C	19.2			8.8	1.1	0.032	1.56		15.0	
15C1 Nac		Mollusk	*Mercenaria Mercenaria*	2	Clams	Growth experiment	A >> C	18.7			9.1	1.3	< LD	1.58		15.0	
23A1 Nac		Mollusk	*Mercenaria Mercenaria*	3	Clams	Growth experiment	A >> C	18.8			7.4	1.2	0.028	1.58		23.0	
23C1 Nac		Mollusk	*Mercenaria Mercenaria*	4	Clams	Growth experiment	A >> C	17.2			8.3	1.7	< LD	1.69		23.0	
30A1 Nac		Mollusk	*Mercenaria Mercenaria*	5	Clams	Growth experiment	A >> C	18.1			7.1	1.0	< LD	2.02		30.0	
30C2 Nac		Mollusk	*Mercenaria Mercenaria*	6	Clams	Growth experiment	A >> C	17.3			7.4	0.9	0.027	1.63		30.0	
30C1 Nac		Mollusk	*Mercenaria Mercenaria*	7	Clams	Growth experiment	A >> C	17.6			7.3	1.6	0.021	1.83		30.0	
PM1	Outer Layer	Mollusk	*Pecten Maximus*	1	Scallop	Growth experiment	C >> A	32.1			25.3	6.5	< LD	1.37		10.8	
PM2	Outer Layer	Mollusk	*Pecten Maximus*	2	Scallop	Growth experiment	C >> A	32.8								10.8	
PM3	Outer Layer	Mollusk	*Pecten Maximus*	3	Scallop	Growth experiment	C >> A	34.5			21.1	6.3	< LD	1.55		10.8	
PM4	Outer Layer	Mollusk	*Pecten Maximus*	4	Scallop	Growth experiment	C >> A	32.6			20.0	9.5	< LD	1.44		15.5	
PM5	Outer Layer	Mollusk	*Pecten Maximus*	5	Scallop	Growth experiment	C >> A	32.1			24.9	5.8	0.025	1.31		15.5	
PM6	Outer Layer	Mollusk	*Pecten Maximus*	6	Scallop	Growth experiment	C >> A	32.6			20.8	5.2	< LD	1.49		15.5	
PM7	Outer Layer	Mollusk	*Pecten Maximus*	7	Scallop	Growth experiment	C >> A									18.0	
PM8	Outer Layer	Mollusk	*Pecten Maximus*	8	Scallop	Growth experiment	C >> A	35.1			15.4	9.8	< LD	1.54		18.0	
PM9	Outer Layer	Mollusk	*Pecten Maximus*	9	Scallop	Growth experiment	C >> A	35.2			22.8	10.9	< LD	1.39		18.0	
PM10	Outer Layer	Mollusk	*Pecten Maximus*	10	Scallop	Growth experiment	C >> A	34.5			24.1	8.2	< LD	1.64		20.2	
PM11	Outer Layer	Mollusk	*Pecten Maximus*	11	Scallop	Growth experiment	C >> A	34.1			22.9	8.3	0.047	1.34		20.2	
PM12	Outer Layer	Mollusk	*Pecten Maximus*	12	Scallop	Growth experiment	C >> A	34.3			19.4	9.3	< LD	1.27		20.2	
ME1	Outer Layer	Mollusk	*Mytilus Eduli*	1	Mussel	Growth experiment	C >> A	37.1			21.4	3.0	< LD	1.48		10.7	
ME2	Outer Layer	Mollusk	*Mytilus Eduli*	2	Mussel	Growth experiment	C >> A	34.9			22.7	2.7	< LD	1.60		10.7	
ME3	Outer Layer	Mollusk	*Mytilus Eduli*	3	Mussel	Growth experiment	C >> A	33.3			23.0	3.6	< LD	1.39		10.7	
ME4	Outer Layer	Mollusk	*Mytilus Eduli*	4	Mussel	Growth experiment	C >> A	37.1			18.4	2.8	< LD	1.17		12.0	
ME5	Outer Layer	Mollusk	*Mytilus Eduli*	5	Mussel	Growth experiment	C >> A				12.4	2.9	< LD	1.02		12.0	
ME6	Outer Layer	Mollusk	*Mytilus Eduli*	6	Mussel	Growth experiment	C >> A									12.0	
ME7	Outer Layer	Mollusk	*Mytilus Eduli*	7	Mussel	Growth experiment	C >> A	36.5								15.6	
ME8	Outer Layer	Mollusk	*Mytilus Eduli*	8	Mussel	Growth experiment	C >> A	37.0			18.8	4.6	< LD	1.08		15.5	
ME9	Outer Layer	Mollusk	*Mytilus Eduli*	9	Mussel	Growth experiment	C >> A									15.5	
ME10	Outer Layer	Mollusk	*Mytilus Eduli*	10	Mussel	Growth experiment	C >> A	38.2			15.4	4.3	< LD	1.18		18.4	
ME11	Outer Layer	Mollusk	*Mytilus Eduli*	11	Mussel	Growth experiment	C >> A	38.2			15.8	4.0	< LD	1.33		18.4	
ME12	Outer Layer	Mollusk	*Mytilus Eduli*	12	Mussel	Growth experiment	C >> A	39.1			13.1	5.3	< LD	1.24		18.0	
ME13	Outer Layer	Mollusk	*Mytilus Eduli*	13	Mussel	Growth experiment	C >> A	37.5			16.8	6.5	< LD	1.31		18.0	
ME14	Outer Layer	Mollusk	*Mytilus Eduli*	14	Mussel	Growth experiment	C >> A	35.4			20.8	9.8	< LD	1.10		20.2	
ME15	Outer Layer	Mollusk	*Mytilus Eduli*	15	Mussel	Growth experiment	C >> A	36.8			19.1	7.2	< LD	1.28		20.2	
ME16	Outer Layer	Mollusk	*Mytilus Eduli*	16	Mussel	Growth experiment	C >> A	39.6			12.8	6.2	< LD	1.15		20.2	

[1]Dominant mineralogy: A refers to 100% aragonite, A >> C to more than 90% aragonite, A > C between 90 and 50% aragonite, A=C equivalent proportion of aragonite and calcite, C > A between 50 and 10% aragonite, C >> A less than 10% aragonite and C to 100% calcite.

[2]For field collected specimens, growth temperatures (in °C) correspond to average temperatures for the three warmest months.
[3]Average annual temperature (in °C)
[*] Temperature calculated using Oxygen isotope data and the relationship between d18O and temperature from Ullmann et al., (2010)

Figure captions:

Figure 1: Map representing the location and name of all the field-collected samples from this study. A. America, B. East Asia, Oceania and Antarctica, and C. Europe

Figure 2: Schematic showing the various types of sampling used in this study (bulk and specific layers) for mussels, clams, oysters, and brachiopods.

Figure 3: A) Sr/Ca of the biogenic carbonates from this study as a function of Mg/Ca. Corals (Sr/Ca > 8) are not plotted on this figure. Data collected in this study are consistent with expectations based on mineralogy (higher Sr/Ca and lower Mg/Ca for aragonite compared to calcite). The three points surrounded by a circle have very high Sr/Ca compared to other samples and are excluded from further discussion because the exact mineralogical composition of these samples is not known. B) Li/Ca of the biogenic carbonates as a function of Mg/Ca.

Figure 4: (A) Li isotope composition of modern carbonates, organized by phylum and mineralogy. Small transparent points (for mollusks and corals) correspond to all data for each phylum. Each large data marker corresponds to the average value for one specimen. Data from corals (Marriott et al., 2004a; Rollion-Bard et al., 2009), planktic foraminifera (Hathorne and James, 2006; Marriott et al., 2004a; Misra and Froelich, 2009; Rollion-Bard et al., 2009), and benthic foraminifera (Marriott et al., 2004b) are from previously published literature. (B) Li/Ca ratio of modern carbonates, organized by phylum and mineralogy. Each large data marker corresponds to the average value for one specimen. Each small data marker corresponds to an individual measurement. Horizontal bars correspond to the maximum and minimum value for all data for each phylum. Data for corals (Hathorne et al., 2013; Marriott et al., 2004b; Montagna et al., 2014; Rollion-Bard et al., 2009; Rollion-Bard and Blamart, 2015), planktic and benthic foraminifera (Hall et al., 2005; Hall and Chan, 2004; Hathorne and James, 2006; Misra and Froelich, 2012), and red algae (Darrenougue et al., 2014) are

from previous studies. Data from mollusks and brachiopods also include previously published data in addition to results from this study (Delaney et al., 1989; Füllenbach et al., 2015; Thébault et al., 2009; Thébault and Chauvaud, 2013). Skeletal organisms with the highest Li/Ca ratio are high-Mg calcite like red algae (60 to 110 μmol.mol^{-1}; Darrenougue et al., 2014), low-Mg calcitic mollusks (20 to 250 μmol.mol^{-1}; Füllenbach et al., 2015; Thébault and Chauvaud, 2013), and brachiopods (20 to 50 μmol.mol^{-1}; Delaney et al., 1989). Aragonitic mollusks and benthic foraminifera have the lowest reported Li/Ca ratios among skeletal organisms, between 2 and 11 μmol.mol^{-1} (Hall and Chan, 2004; Thébault et al., 2009).

Figure 5: A) Li isotope composition as a function of the temperature for mollusks grown at various temperatures. The small black markers correspond to the inorganic calcite precipitation experiments at various temperature while the small red ones represent abiogenic precipitation experiments at varying salinity (Marriott et al., 2004a). B) Li isotope composition as a function of the growth temperature for modern field-collected biogenic mollusks, brachiopods, and echinoderms from this study. All data correspond to the mean of all the measurements of a single specimen. The initials correspond to the genera and species name. C) Li/Ca ratio of brachiopods as a function of the annual temperature. Data from Delaney et al. (1989) for brachiopods and inorganic experimental data from Marriott et al. (2004) are also represented.

Figure 6: Example of intra-shell Li isotope variability for the species *Mytilus californianus*. (A) Sampling locations shown by the red dots on left figure. (B) δ^7Li varies as a function of aragonite percentage in the shell

Figure 7: $\Delta^7Li_{physiol}$ values as a function of A) $\beta^{Li}{}_{25°C}$ values (Li/Ca ratio normalized to Li/Ca of inorganic carbonate at 25°C) and B) $\beta^{Li}{}_{T}$ values (Li/Ca ratio normalized to Li/Ca of inorganic carbonate at the corresponding growth temperature). The hand-drawn dotted circles correspond to each taxonomic group. C) Also shown for comparison the δ^7Li as a function of the Li/Ca (in μmol.mol^{-1}) for biogenic, inorganic and cultured experiment carbonates.

Figure 8: (A) Δ^7Li_{physio} values as a function of $\beta^{Li}{}_{25°C}$ values (Li/Ca ratio normalized to Li/Ca of inorganic carbonate at 25°C) for mollusks. Calcite mollusks define a negative trend in this space and this trend can be fitted with either a steady-state open system fractionation (black line) or a Rayleigh fractionation model (grey line), both with an $r^2 = 0.64$ (excluding the sample having the highest $\beta^{Li}{}_{25°C}$ value). The numbers along the model curves correspond to the proportion of Li remaining in the calcification reservoir before precipitation of the shell. (B) Negative relationship between Δ^7Li_{physio} and Mg/Ca in calcitic mollusks. Shells having the highest Δ^7Li_{physio} values also have the lowest Mg/Ca ratio.

Sample name	Sample type	Phyllum	Species	Specimen #	Common name	Sampling location
Field-collected Mollusk samples						
57-12	Mixed	Mollusk	*Chlamys cheritata*		Scallops	Alaska (Kachemak Bay) USA
167501	Mixed	Mollusk	*Chlamys hastata*		Scallops	Newport Beach, CA USA
53819	Mixed	Mollusk	*Chlamys squamosus*		Scallops	Zamboanga, Philippine Islands
170315	Mixed	Mollusk	*Chione californiensis*		Clams	San Pedro, CA USA
170315	Inner Layer	Mollusk	*Chione californiensis*		Clams	San Pedro, CA USA
170315	Interm Layer	Mollusk	*Chione californiensis*		Clams	San Pedro, CA USA
86-29	Mixed (ext)	Mollusk	*Chione subimbricata*		Clams	Costa Rica (Golfo de Papagayo)
86-29	Outer Layer	Mollusk	*Chione subimbricata*		Clams	Costa Rica (Golfo de Papagayo)
72-84	Mixed	Mollusk	*Chione subrugosa*		Clams	Peru (Puerto Pizzaro)
72-84	Inner Layer	Mollusk	*Chione subrugosa*		Clams	Peru (Puerto Pizzaro)
72-84	Outer Layer	Mollusk	*Chione subrugosa*		Clams	Peru (Puerto Pizzaro)
50338	Inner Layer	Mollusk	*Tridacna Maxima*		Clams	Guam, Mariana Islands
50338	Outer Layer	Mollusk	*Tridacna Maxima*		Clams	Guam, Mariana Islands
MT1 PNG		Mollusk	*Tridacna Gigas*		Clams	Cocos, Island, Costa Rica
83-26	Inner Layer	Mollusk	*Mytilus californianus*	1	Mussel	Washington state, USA
83-26	Outer Layer	Mollusk	*Mytilus californianus*	1	Mussel	Washington state, USA
76-39	Front (outer)	Mollusk	*Mytilus californianus*	2	Mussel	Baja Calif, Mexico
76-39	Mixed Middle	Mollusk	*Mytilus californianus*	2	Mussel	Baja Calif, Mexico
76-39	Mixed Hinge	Mollusk	*Mytilus californianus*	2	Mussel	Baja Calif, Mexico
76-39	Inner Layer	Mollusk	*Mytilus californianus*	2	Mussel	Baja Calif, Mexico
76-39	Outer Layer	Mollusk	*Mytilus californianus*	2	Mussel	Baja Calif, Mexico
AN88	Mixed	Mollusk	*Laternula Elliptica*		Clams	Terra Nova Bay, Antarctica
	Mixed	Mollusk	*Adamussium Colbecki*		Scallop	Ross sea, Edmundson, Antarctica
	Mixed Top	Mollusk	*Turritella*		Gastropod	
	Mixed Back	Mollusk	*Turritella*		Gastropod	
112-72		Mollusk	*Crassostrea gigas*	1	Oyster	Washington state, USA

112-72	Inner Layer	Mollusk	*Crassostrea gigas*	1	Oyster	Washington state, USA
112-72	Outer Layer	Mollusk	*Crassostrea gigas*	1	Oyster	Washington state, USA
110-50		Mollusk	*Crassostrea gigas*	2	Oyster	Tomales Bay, CA, USA
110-50	Outer Layer	Mollusk	*Crassostrea gigas*	2	Oyster	Tomales Bay, CA, USA
66-117		Mollusk	*Crassostrea gigas*	3	Oyster	Gulf of Guayaquil, Ecuador
ofl01	foliate layers	Mollusk	*Crassostrea gigas*	4	Oyster	List Tidal Basin Germany
ofl02	foliate layers	Mollusk	*Crassostrea gigas*	4	Oyster	List Tidal Basin Germany
ofl03	foliate layers	Mollusk	*Crassostrea gigas*	4	Oyster	List Tidal Basin Germany
ofl04	foliate layers	Mollusk	*Crassostrea gigas*	4	Oyster	List Tidal Basin Germany
ofl05	foliate layers	Mollusk	*Crassostrea gigas*	4	Oyster	List Tidal Basin Germany
ofl06	foliate layers	Mollusk	*Crassostrea gigas*	4	Oyster	List Tidal Basin Germany
ofl07	foliate layers	Mollusk	*Crassostrea gigas*	4	Oyster	List Tidal Basin Germany
ofl08	foliate layers	Mollusk	*Crassostrea gigas*	4	Oyster	List Tidal Basin Germany
ofl09	foliate layers	Mollusk	*Crassostrea gigas*	4	Oyster	List Tidal Basin Germany
ofl10	foliate layers	Mollusk	*Crassostrea gigas*	4	Oyster	List Tidal Basin Germany
ofl11	foliate layers	Mollusk	*Crassostrea gigas*	4	Oyster	List Tidal Basin Germany
och01	chalky substance	Mollusk	*Crassostrea gigas*	4	Oyster	List Tidal Basin Germany
och02	chalky substance	Mollusk	*Crassostrea gigas*	4	Oyster	List Tidal Basin Germany
och03	chalky substance	Mollusk	*Crassostrea gigas*	4	Oyster	List Tidal Basin Germany
och04	chalky substance	Mollusk	*Crassostrea gigas*	4	Oyster	List Tidal Basin Germany
och05	chalky substance	Mollusk	*Crassostrea gigas*	4	Oyster	List Tidal Basin Germany
och06	chalky substance	Mollusk	*Crassostrea gigas*	4	Oyster	List Tidal Basin Germany
och07	chalky substance	Mollusk	*Crassostrea gigas*	4	Oyster	List Tidal Basin Germany
och08	chalky substance	Mollusk	*Crassostrea gigas*	4	Oyster	List Tidal Basin Germany

och09	chalky substance	Mollusk	*Crassostrea gigas*	4	Oyster	List Tidal Basin Germany
och10	chalky substance	Mollusk	*Crassostrea gigas*	4	Oyster	List Tidal Basin Germany
och11	chalky substance	Mollusk	*Crassostrea gigas*	4	Oyster	List Tidal Basin Germany
Field-collected Brachiopod samples						
	Mixed	Brachiopoda	*Campages mariae*		Brachiopod	Aliguay Island, Philippines
	Mixed	Brachiopoda	*Laqueus Rubellus*		Brachiopod	Sagami Bay, Japan
	Mixed	Brachiopoda	*Terebratulina Transversa*		Brachiopod	Puget Sound, Nr. Friday, Harbor, Washington USA
	Back-Dorsal	Brachiopoda	*Terebratulina Transversa*		Brachiopod	Puget Sound, Nr. Friday, Harbor, Washington USA
	Back-Ventral	Brachiopoda	*Terebratulina Transversa*		Brachiopod	Puget Sound, Nr. Friday, Harbor, Washington USA
	Front-Dorsal	Brachiopoda	*Terebratulina Transversa*		Brachiopod	Puget Sound, Nr. Friday, Harbor, Washington USA
	Mixed	Brachiopoda	*Notosaria nigricans*		Brachiopod	South Island, New Zealand
	Mixed	Brachiopoda	*Frenulina sanguinolenta*		Brachiopod	Mactan Island, Philippines
Field-collected Echinoderm samples						
	Mixed	Sea Urchin	*Strongylocentrotus fransiscanus*		Urchins	Leo Carillo, CA, USA
	Mixed	Sea Urchin	*Strongylocentrotus purpuratus*		Urchins	Leo Carillo, CA, USA
	Mixed	Sea Urchin	*Dendraster*		Urchins	Morro Bay, CA, USA
Growth experiment mollusks samples						
15A2 Nac		Mollusk	*Mercenaria Mercenaria*	1	Clams	Growth experiment
15C1		Mollusk	*Mercenaria Mercenaria*	2	Clams	Growth experiment

Nac 23A1 Nac		Mollusk	*Mercenaria Mercenaria*	3	Clams	Growth experiment
Nac 23C1 Nac		Mollusk	*Mercenaria Mercenaria*	4	Clams	Growth experiment
Nac 30A1 Nac		Mollusk	*Mercenaria Mercenaria*	5	Clams	Growth experiment
Nac 30C2 Nac		Mollusk	*Mercenaria Mercenaria*	6	Clams	Growth experiment
Nac 30C1 Nac		Mollusk	*Mercenaria Mercenaria*	7	Clams	Growth experiment
PM1	Outer Layer	Mollusk	*Pecten Maximus*	1	Scallop	Growth experiment
PM2	Outer Layer	Mollusk	*Pecten Maximus*	2	Scallop	Growth experiment
PM3	Outer Layer	Mollusk	*Pecten Maximus*	3	Scallop	Growth experiment
PM4	Outer Layer	Mollusk	*Pecten Maximus*	4	Scallop	Growth experiment
PM5	Outer Layer	Mollusk	*Pecten Maximus*	5	Scallop	Growth experiment
PM6	Outer Layer	Mollusk	*Pecten Maximus*	6	Scallop	Growth experiment
PM7	Outer Layer	Mollusk	*Pecten Maximus*	7	Scallop	Growth experiment
PM8	Outer Layer	Mollusk	*Pecten Maximus*	8	Scallop	Growth experiment
PM9	Outer Layer	Mollusk	*Pecten Maximus*	9	Scallop	Growth experiment
PM10	Outer Layer	Mollusk	*Pecten Maximus*	10	Scallop	Growth experiment
PM11	Outer Layer	Mollusk	*Pecten Maximus*	11	Scallop	Growth experiment
PM12	Outer Layer	Mollusk	*Pecten Maximus*	12	Scallop	Growth experiment
ME1	Outer Layer	Mollusk	*Mytilus Eduli*	1	Mussel	Growth experiment
ME2	Outer Layer	Mollusk	*Mytilus Eduli*	2	Mussel	Growth experiment
ME3	Outer Layer	Mollusk	*Mytilus Eduli*	3	Mussel	Growth experiment
ME4	Outer Layer	Mollusk	*Mytilus Eduli*	4	Mussel	Growth experiment
ME5	Outer Layer	Mollusk	*Mytilus Eduli*	5	Mussel	Growth experiment
ME6	Outer Layer	Mollusk	*Mytilus Eduli*	6	Mussel	Growth experiment

ME7	Outer Layer	Mollusk	*Mytilus Eduli*	7	Mussel	Growth experiment
ME8	Outer Layer	Mollusk	*Mytilus Eduli*	8	Mussel	Growth experiment
ME9	Outer Layer	Mollusk	*Mytilus Eduli*	9	Mussel	Growth experiment
ME10	Outer Layer	Mollusk	*Mytilus Eduli*	10	Mussel	Growth experiment
ME11	Outer Layer	Mollusk	*Mytilus Eduli*	11	Mussel	Growth experiment
ME12	Outer Layer	Mollusk	*Mytilus Eduli*	12	Mussel	Growth experiment
ME13	Outer Layer	Mollusk	*Mytilus Eduli*	13	Mussel	Growth experiment
ME14	Outer Layer	Mollusk	*Mytilus Eduli*	14	Mussel	Growth experiment
ME15	Outer Layer	Mollusk	*Mytilus Eduli*	15	Mussel	Growth experiment
ME16	Outer Layer	Mollusk	*Mytilus Eduli*	16	Mussel	Growth experiment